Nucleosynthesis of light and heavy elements across the Galaxy

Candidate: Diego Vescovi

Advisors: Sergio Cristallo, Marica Branchesi

PhD Thesis Defense
GSSI, 2 February 2021

Outline

- Solar neutrinos and luminosity constraint in the era of precision solar physics
- Presolar grains and magnetic-buoyancy-induced mixing in Asymptotic Giant Branch (AGB) stars
- Kilonovae and production of very light elements in Neutron Star Mergers (NSMs)

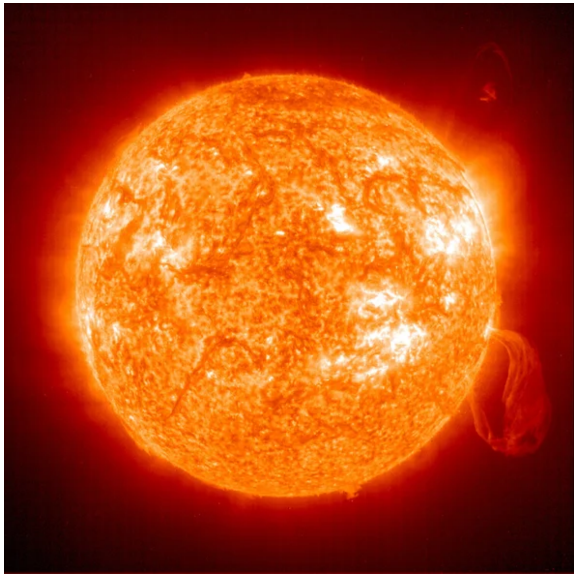
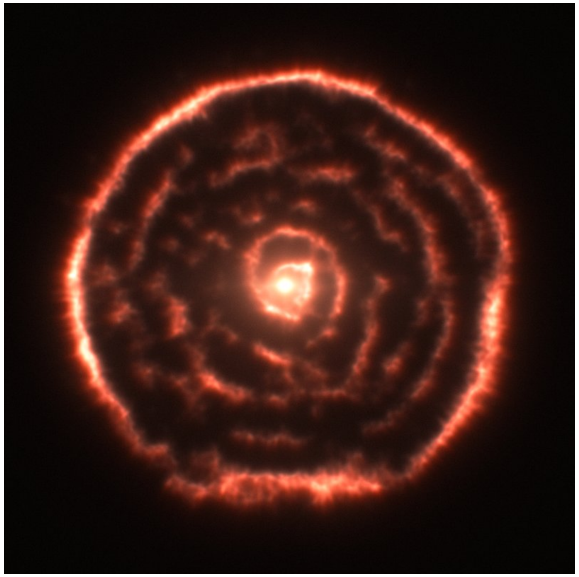
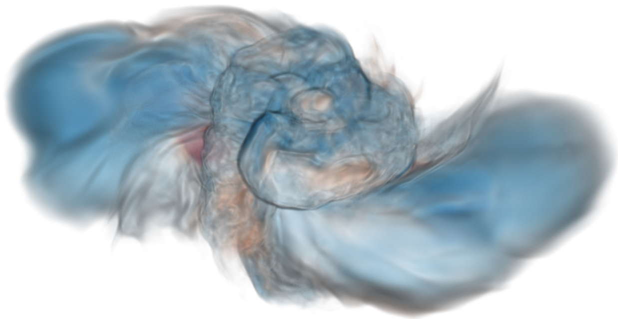

Solar neutrinos and luminosity constraint in the era of precision solar physics

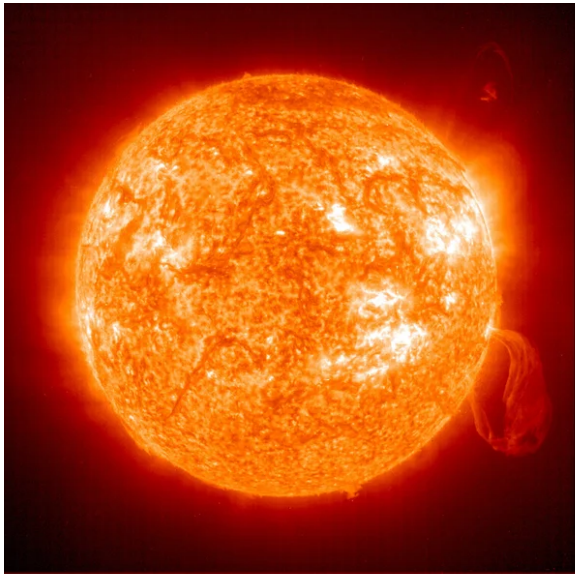

The Sun: nuclear processes and neutrinos

- The Sun is powered by nuclear reactions that transform H into ^{4}He

$$4p + 2e^- \rightarrow {}^4\mathrm{He} + 2\nu_e + 26.731\,\mathrm{MeV}$$

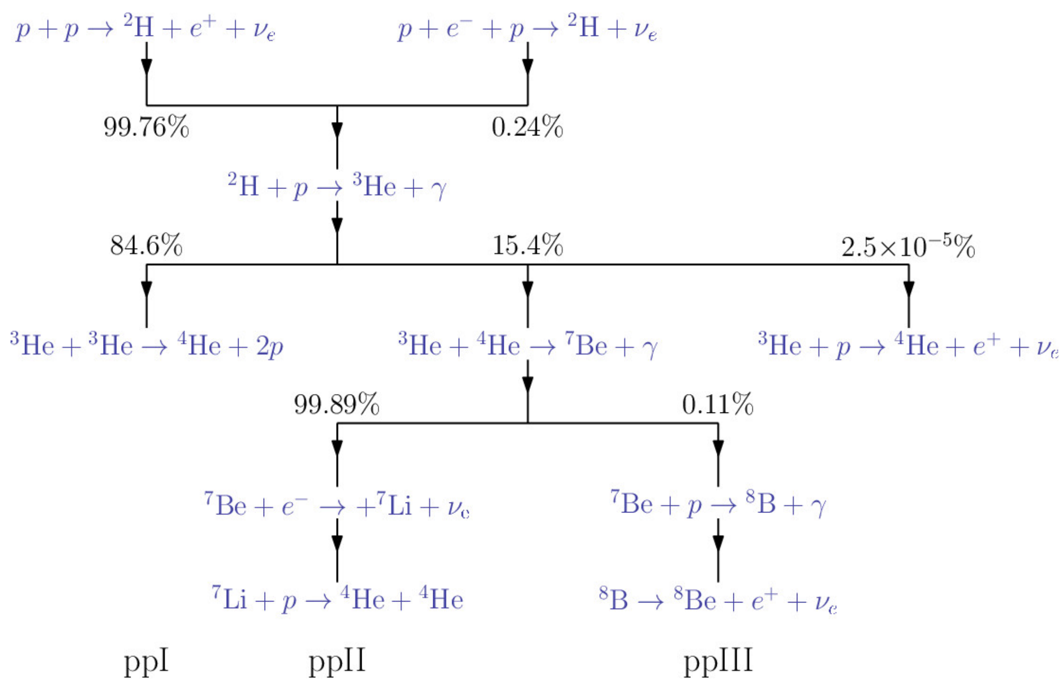

- Two main sequences of reactions:

  1) **pp chain**

  2) **CNO cycle**

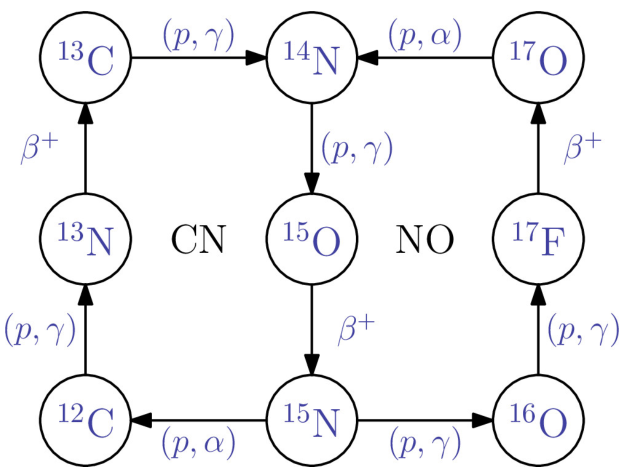

Products: <u>neutrinos</u>

→ pp, pep, hep, ^{7}Be, ^{8}B, ^{13}N, ^{15}C, ^{17}F

Standard Solar Model (SSM)

"*A SSM is one which reproduces, within uncertainties, the observed properties of the Sun, by adopting a set of physical and chemical inputs chosen within the range of their uncertainties*" (Bahcall, 1995)

- Evolve a model with 1 $M_\odot$ starting from a chemically homogeneous model to present solar age with the best available micro- and macro-physics

→ **Match $R_\odot$, $L_\odot$, and $(Z/X)_\odot$ to better than one part in 10^{-5}**

- Predictions:

  1) Physical quantities

  2) Chemical profiles

  3) Helioseismic quantities

  4) Neutrino fluxes

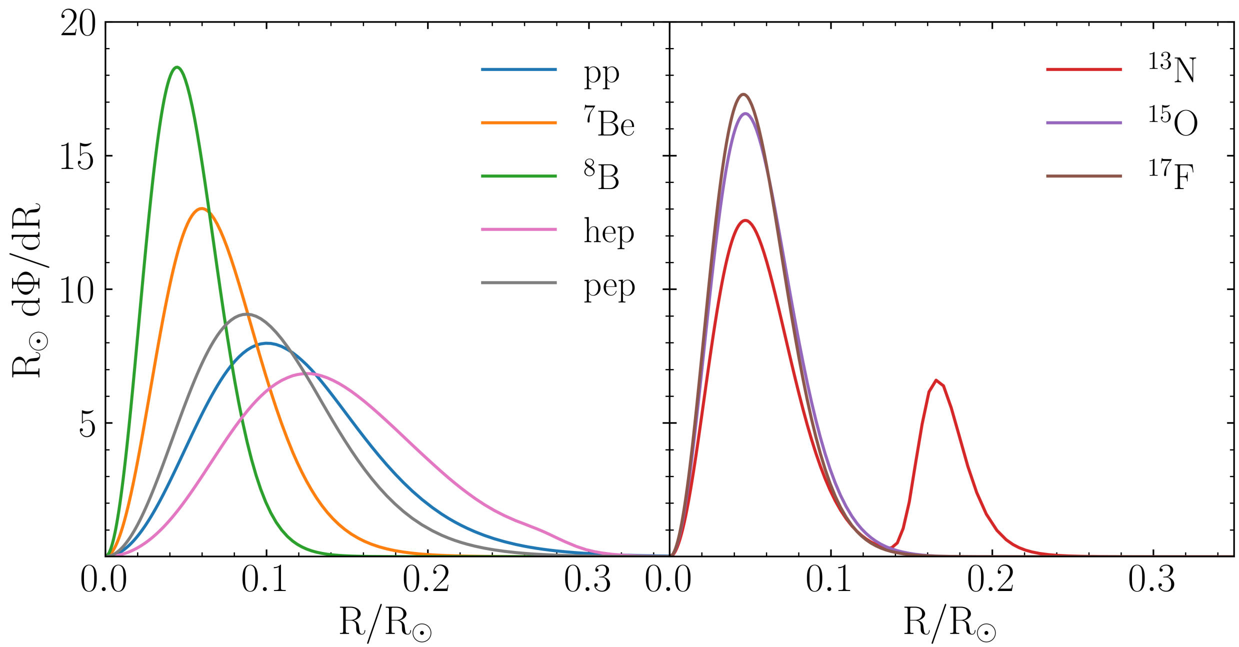

SSM: the solar abundance problem

- SSM can be then validated by observational constraints → **solar neutrino fluxes** and **helioseismic** measurements
- New generation of spectroscopic studies yield a solar metallicity lower than older results
- Theoretical predictions of SSMs adopting low metallicity surface compositions fail in reproducing all helioseismic determinations of solar properties

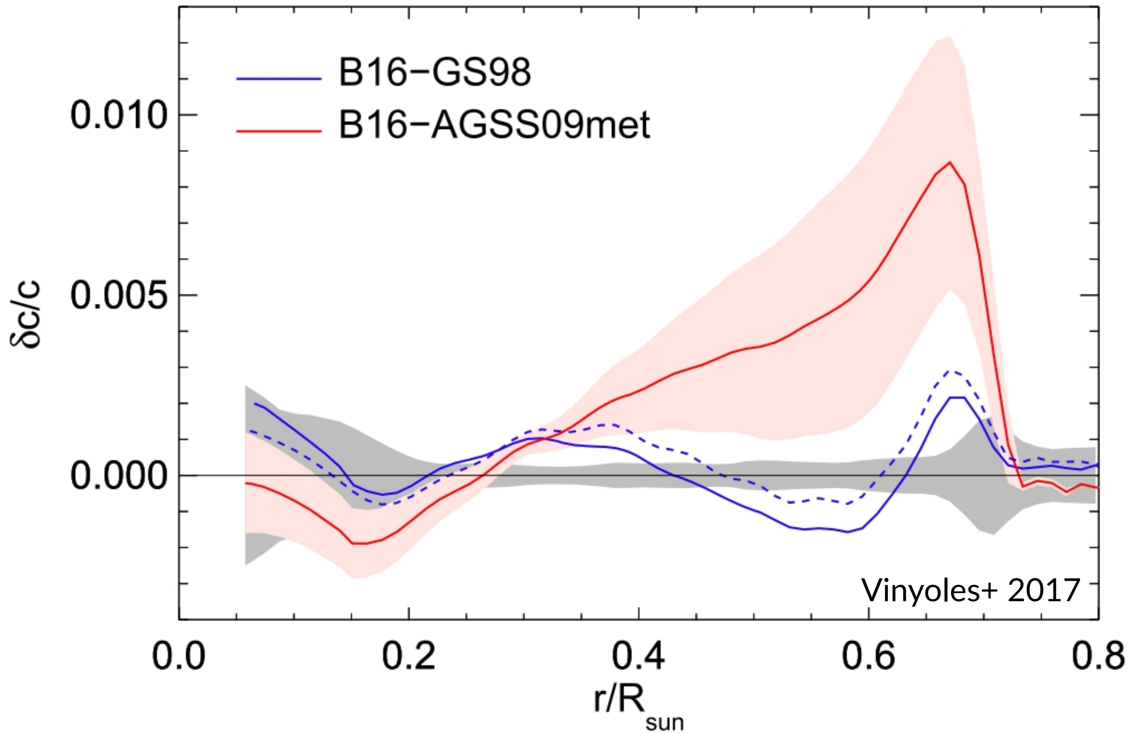

SSMs: solutions?

- Solutions:

  1) <u>Increase of the heavy-element admixture</u>

  2) <u>Increase of the radiative opacitiy</u> at the base of the convective envelope

- The degeneracy between radiative opacity and solar composition can be removed by **measuring the neutrino fluxes produced in the CNO cycle**, i.e. the CNO burning rate

- CNO neutrinos have low energies (~ MeV) and are produced in the same energy region of neutrinos from the pp chain

➔ <u>Experimental challenge</u>

Gallo Rosso+ 2018

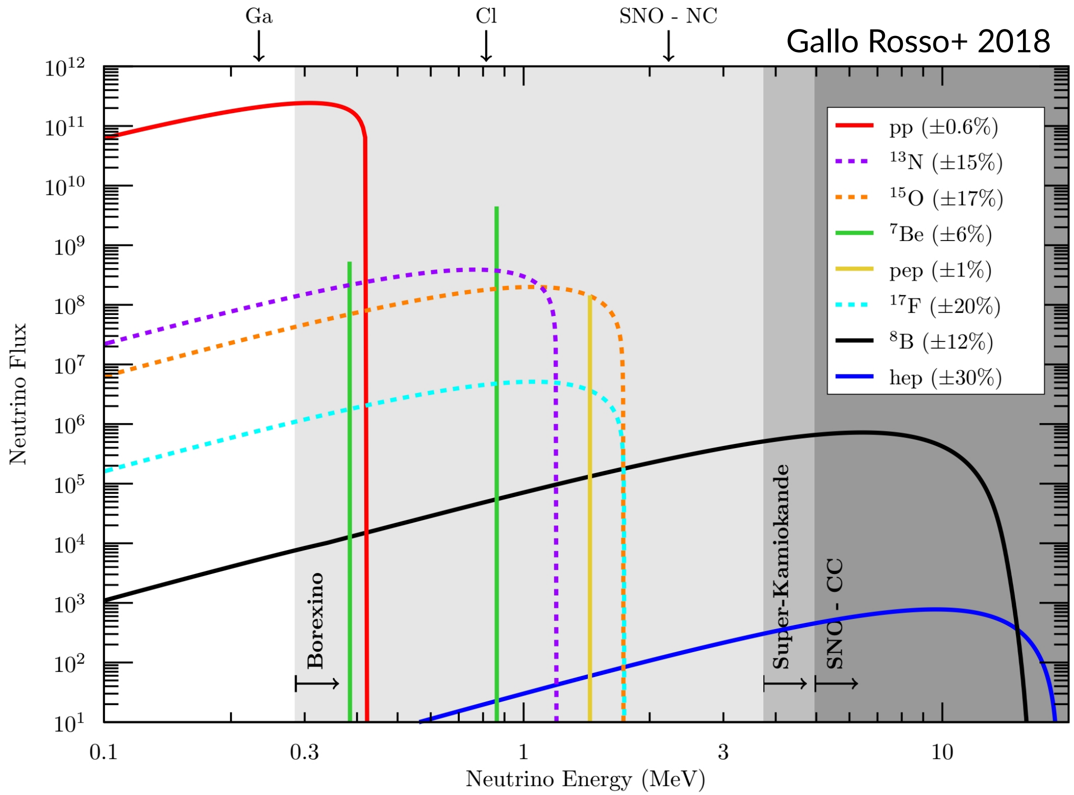

Constraints from neutrinos

- Experimental measured fluxes ($\Phi_i = \varphi_i \times 10^{\gamma_i}\ \mathrm{cm}^2/\mathrm{s}$) agree with SSM results

Vescovi+, JPhG 2021

Flux	γ_i	φ_i GS98	φ_i PLJ14	Experimental results	Source
Φ_{pp}	10	$\boxed{5.99(1 \pm 0.01)}$	$\boxed{6.01(1 \pm 0.01)}$	$\boxed{6.1(1 \pm 0.1)}$	BX
Φ_{pep}	8	$1.42(1 \pm 0.02)$	$1.43(1 \pm 0.02)$	$1.27(1 \pm 0.17)$	BX
Φ_{Be}	9	$\boxed{4.73(1 \pm 0.12)}$	$\boxed{4.52(1 \pm 0.12)}$	$\boxed{4.99(1 \pm 0.03)}$	BX
Φ_{B}	6	$\boxed{5.52(1 \pm 0.24)}$	$\boxed{5.01(1 \pm 0.24)}$	$\boxed{5.41(1 \pm 0.016)}$	SK
Φ_{hep}	3	$8.15(1 \pm 0.30)$	$8.28(1 \pm 0.30)$	$8(1 \pm 2)$	SNO
Φ_{N}	8	$2.87(1 \pm 0.30)$	$2.58(1 \pm 0.29)$	—	—
Φ_{O}	8	$2.13(1 \pm 0.36)$	$1.86(1 \pm 0.35)$	—	—
Φ_{F}	6	$5.51(1 \pm 0.37)$	$4.04(1 \pm 0.36)$	—	—
Φ_{CNO}	8	$\boxed{5.06(1 \pm 0.32)}$	$\boxed{4.48(1 \pm 0.31)}$	$\boxed{7.0^{+3.0}_{-2.0}}$	BX

- ^{7}Be and ^{8}B neutrino fluxes are probed with high precision → solar core temperature
- What about pp and CNO fluxes?
- Helpful instrument: **luminosity constraint**

The “standard” luminosity constraint

- **Nuclear fusion is responsible for the observed solar luminosity**

→ Gravothermal energy negligible $\quad \Rightarrow \quad L_\odot = L_{\rm nuc} - L_\nu$

→ Local nuclear equilibrium $\quad \Rightarrow \quad L_{\rm nuc} = Q_4 \dot{N}(^4{\rm He})$

$$4p + 2e^- \rightarrow {}^4{\rm He} + 2\nu_{\rm e} + {\rm Q}_4$$

→ Lepton number conservation $\quad \Rightarrow \quad 4\pi {\rm au}^2 \sum_i \Phi_i = 2\dot{N}(^4{\rm He})$

$$L_\odot = Q_4 \underbrace{\frac{4\pi {\rm au}^2 \sum_i \Phi_i}{2}}_{\dot{N}(^4{\rm He})} - \underbrace{4\pi {\rm au}^2 \sum_i \langle E_i \rangle \Phi_i}_{L_\nu} \quad \Rightarrow \quad \boxed{\frac{L_\odot}{4\pi {\rm au}^2} = \sum_i \left(\frac{Q_4}{2} - \langle E_i \rangle \right) \Phi_i}$$

Limits of the standard luminosity constraint

- The total number of both ^{3}He and ^{14}N nuclei in the whole Sun increases with the time
- In the Sun, the gravothermal energy is absorbed to produce an expansion against gravity on a timescale of few Myr

Vescovi+, JPhG 2021

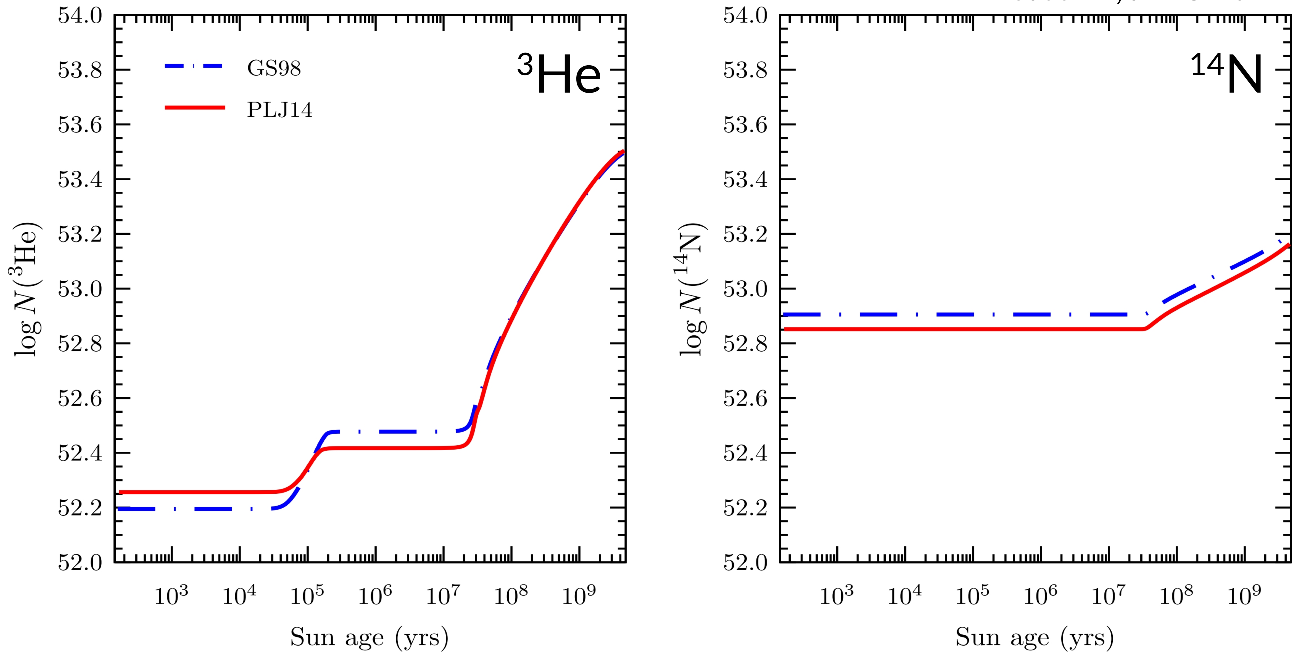

- The standard luminosity constraint is **accurate to better than 1%**
- Extremely precise determination of $L_\odot = 3.8275\,(1 \pm 0.4‰) \times 10^{33}\mathrm{erg/s}$ **requires corrections** to the "standard" form

A new version of the luminosity constraint

- **Not only** nuclear fusion is responsible for the observed solar luminosity

→ Gravothermal energy ➡ $L_\odot = L_{\rm nuc} - L_\nu - L_{\rm g}$

→ Production of more nuclei ➡ $L_{\rm nuc} = \sum_j Q_j \dot{N}(j)$

→ Lepton number conservation ➡ $4\pi {\rm au}^2 \sum_i \Phi_i = \sum_j c_j \dot{N}(j)$

➡ $$\boxed{\frac{1}{4\pi {\rm au}^2}\left(L_\odot + L_{\rm g} + \sum_{j \neq {}^4{\rm He}} L_j\right) = \sum_i \left(\frac{Q_4}{2} - E_i\right)\Phi_i}$$

Where $L_j := \left(\frac{c_j Q_4}{2} - Q_j\right)\dot{N}(j)$ accounts for the corrections due to the isotope *j*

SSM computations

- By making use of SSMs, corrective terms can be evaluated!
- Two solar mixtures → high-metallicity (GS98) and low-metallicity (PLJ14)
- State-of-the-art opacities (OPAL05)
- Latest reaction rates (Solar fusion II + updates)

➔ Relevant corrections: must be of the order of **0.4‰ $L_\odot \simeq 1.5 \times 10^{30}$ erg s^{-1}**

Models	$\dot{N}(^3\mathrm{He})$	$\dot{N}(^{14}\mathrm{N})$	$L_{^3\mathrm{He}}$	$L_{^{14}\mathrm{N}}$	L_g
GS98	$3.29(1 \pm 0.07)$	$2.15(1 \pm 0.13)$	$\boxed{3.39}(1 \pm 0.07)$	$\boxed{0.57}(1 \pm 0.13)$	$\boxed{1.54}(1 \pm 0.04)$
PLJ14	$3.42(1 \pm 0.07)$	$2.07(1 \pm 0.13)$	$\boxed{3.53}(1 \pm 0.07)$	$\boxed{0.55}(1 \pm 0.13)$	$\boxed{1.52}(1 \pm 0.04)$

$\dot{N}(j)$ (units of 10^{35} s^{-1}) and L_j (units of 10^{30} erg s^{-1})

➔ $L_{^3\mathrm{He}}$, $L_{^{14}\mathrm{N}}$, and L_g **do matter** and have small uncertainties

A new version of the luminosity constraint II

$$1 \pm 0.4\,‰ = \frac{1}{\mathcal{F}} \sum_i \left(\frac{Q_4}{2} - \langle E_i \rangle \right) \Phi_i$$

Standard

$$\mathcal{F} = \frac{L_\odot}{4\pi \mathrm{au}^2}$$

$$\mathcal{F} = 8.4946 \times 10^{11}$$

New

$$\mathcal{F} = \frac{L_\odot + L_{^3\mathrm{He}} + L_{^{14}\mathrm{N}} + L_\mathrm{g}}{4\pi \mathrm{au}^2}$$

$$\mathcal{F}(\mathrm{GS98}) = 8.5068 \times 10^{11}$$

$$\mathcal{F}(\mathrm{PLJ14}) = 8.5070 \times 10^{11}$$

- Fixed solar luminosity (by observations) and the three new terms are all positive → number of expected neutrinos increased

- $\mathcal{F}$ increases of ~1.5 ‰

- Negligible dependence on solar composition

Luminosity constraint and the search for CNO neutrinos

It is possible to obtain a constraint on the flux of pp and CNO neutrinos by:

- neglecting $\Phi_{\rm hep}$ (very small)
- adopting $\Phi_{\rm pep}/\Phi_{\rm pp}$ and $\Phi_{\rm O}/\Phi_{\rm N}$ from SSMs
- fixing $\Phi_{\rm Be}$ and $\Phi_{\rm B}$ to the experimental results - known better than theory

$$\rightarrow \quad \boxed{\Phi_{\rm pp} + 1.654\,\Phi_{\rm N} = k\,(1 \pm 2\,‰) \times 10^{10}\,{\rm cm}^{-2}{\rm s}^{-1}}$$

Corrective terms	GS98	PLJ14	Average
None	5.9936	5.9936	5.9936
$L_{^3{\rm He}}$	5.9994	5.9996	5.9995
$L_{^3{\rm He}} + L_{^{14}{\rm N}}$	6.0004	6.0006	6.0005
$L_{^3{\rm He}} + L_{^{14}{\rm N}} + L_{\rm g}$	6.0030	6.0031	6.0031

+1.5 ‰

pp flux and CNO flux

In terms of $\Phi_{\rm CNO} = \Phi_{\rm N} + \Phi_{\rm O} + \Phi_{\rm F}$:

$$\Rightarrow \Phi_{\rm pp} + 0.946\,\Phi_{\rm CNO} = 6.003\,(1 \pm 2\,‰) \times 10^{10}{\rm cm}^{-2}{\rm s}^{-1}$$

- Using $\Phi_{\rm CNO}$ measured by Borexino collaboration

$$\boxed{\Phi_{\rm pp} = 5.937^{+0.023}_{-0.032}{\rm cm}^{-2}{\rm s}^{-1}}$$

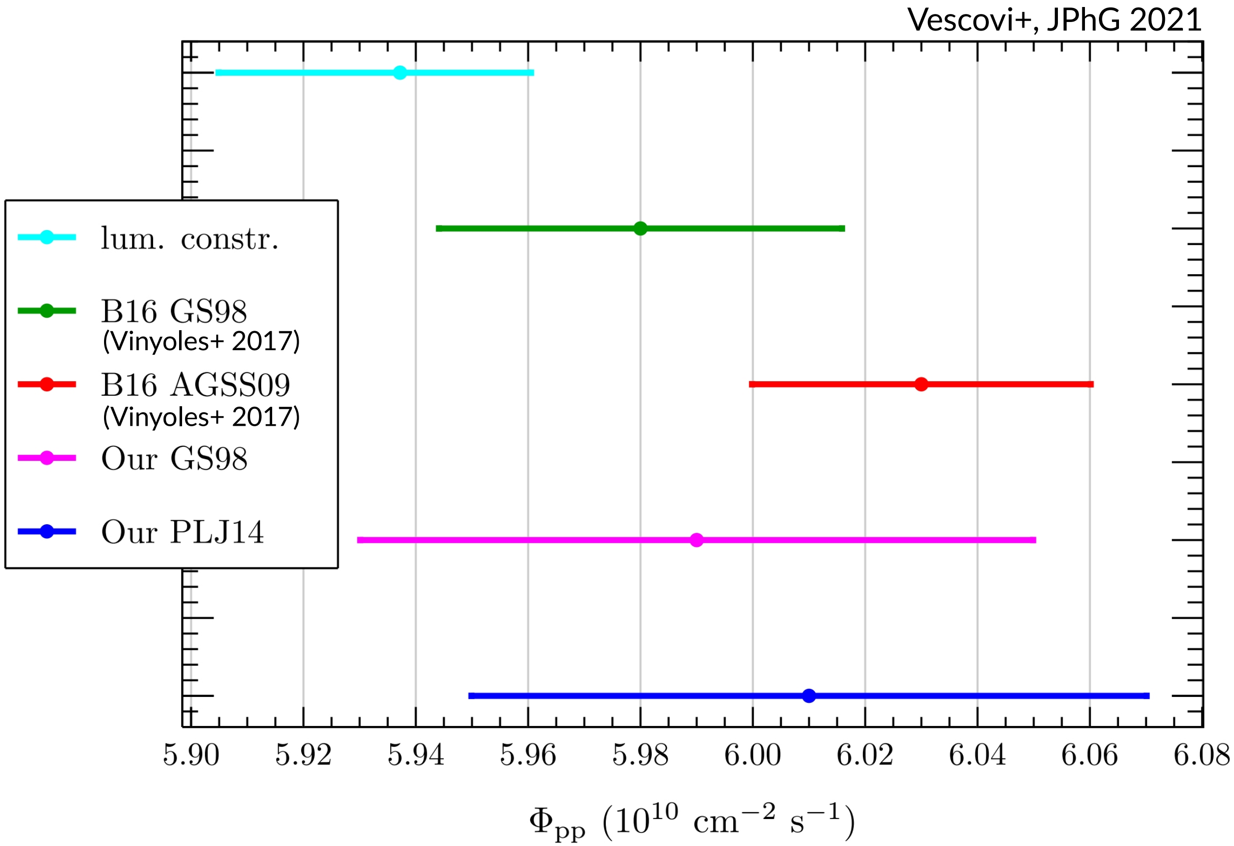

Summary I - Probing metals and CNO in the Sun

Location	Method	Precision
Surface	Observation/ modeling	permil
Convective/radiative interface	Helioseismology	permil
Core	CNO neutrinos	percent

- CNO flux measurement may **solve** the longstanding solar abundance problem
- It relies on the **luminosity constraint** which establishes the best available limits on the rate of creation of pp neutrinos
- Development of a **new version** including corrective terms → non-equilibrium burning of ^{3}He and ^{14}N abundances and gravothermal energy
- Simple relation linking in Φ_{pp} and Φ_{CNO}, independent from solar core metallicity
- Φ_{pp} in better agreement with high-metallicity SSMs

Presolar grains and magnetic-buoyancy-induced mixing in Asymptotic Giant Branch stars

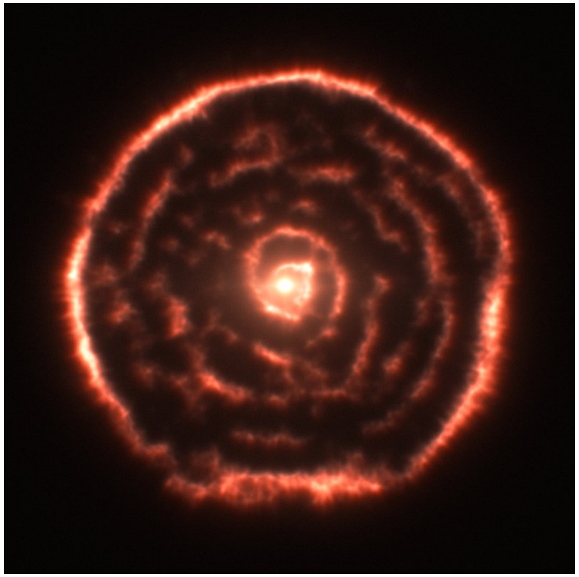

The origin of heavy elements in the Solar System

- Fusion reactions between charged particles
- Neutron capture processes :
  - → **r(apid)-process**
  - → **s(low)-process**

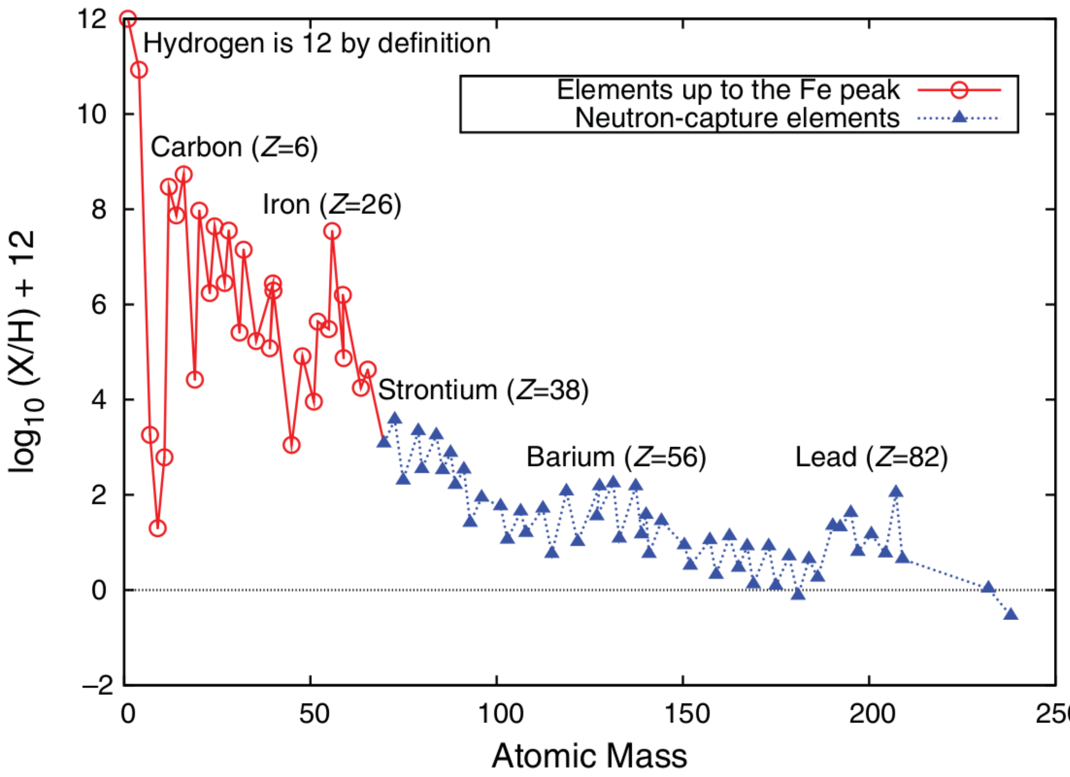

s- and r- process

r-process

High neutron density n_n

- $\tau_{(n,\gamma)} << \tau_{\beta\text{-decay}}$
- Supernovae and compact binary mergers

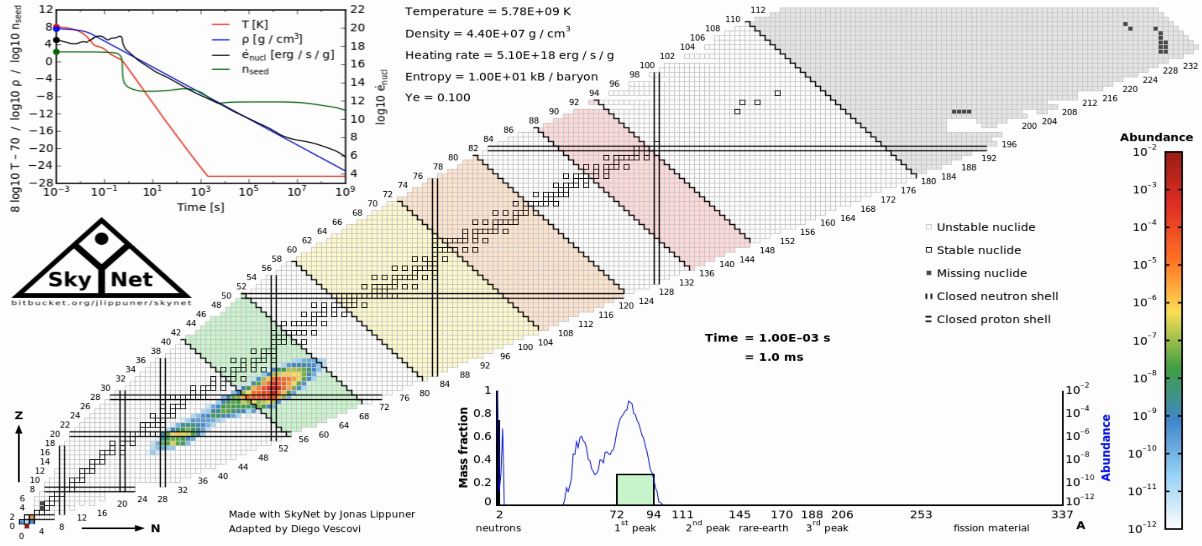

s-process

Mild neutron density n_n

- $\tau_{(n,\gamma)} \gtrsim \tau_{\beta\text{-decay}}$
- Asymptotic Giant Branch (AGB) and massive stars

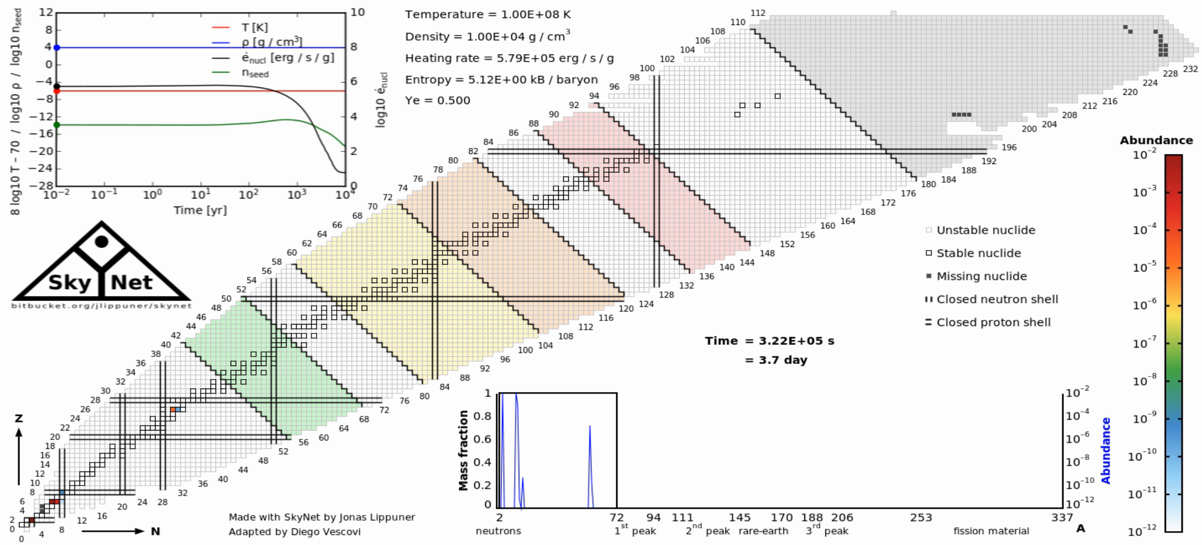

Moving towards the AGB phase

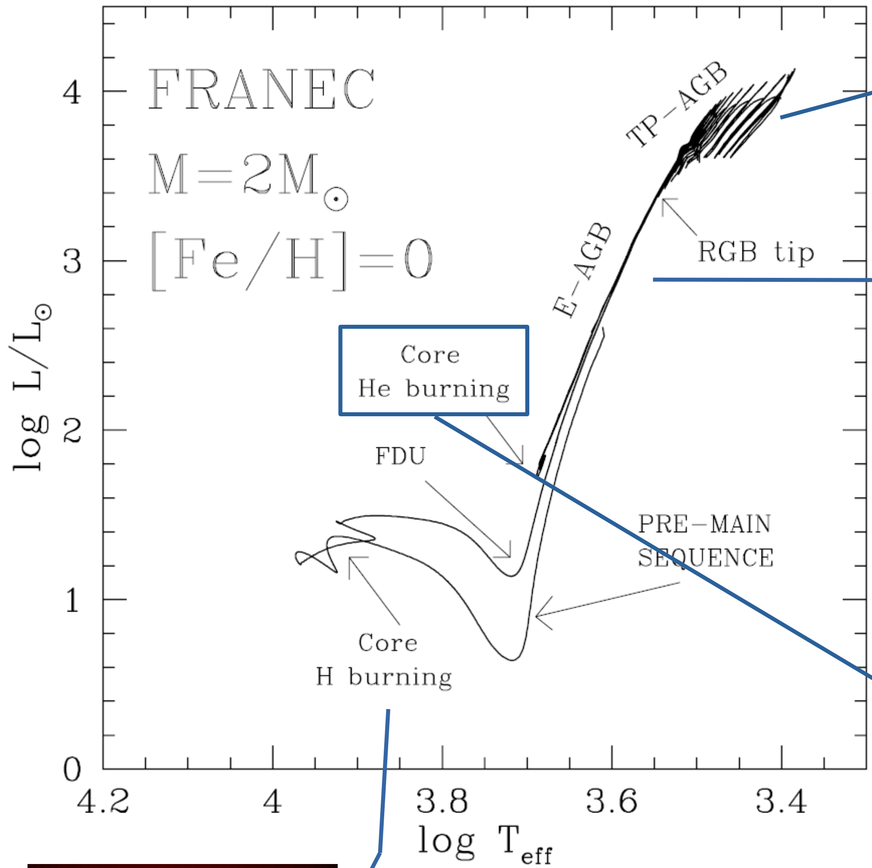

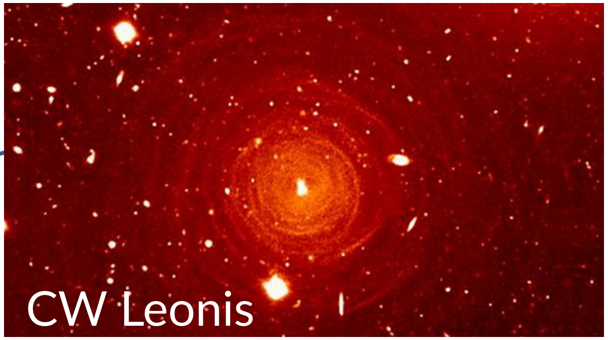

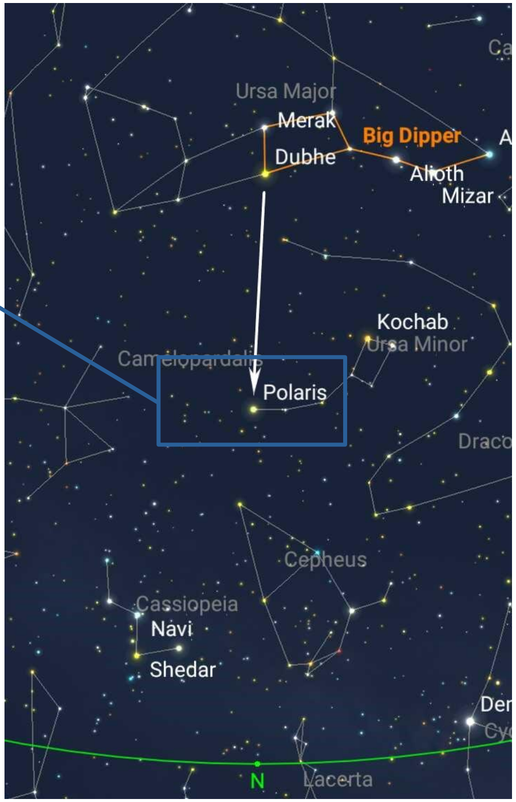

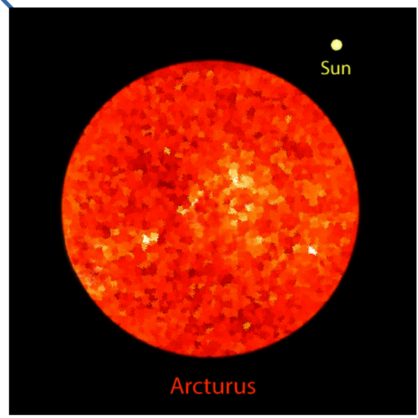

AGB stars

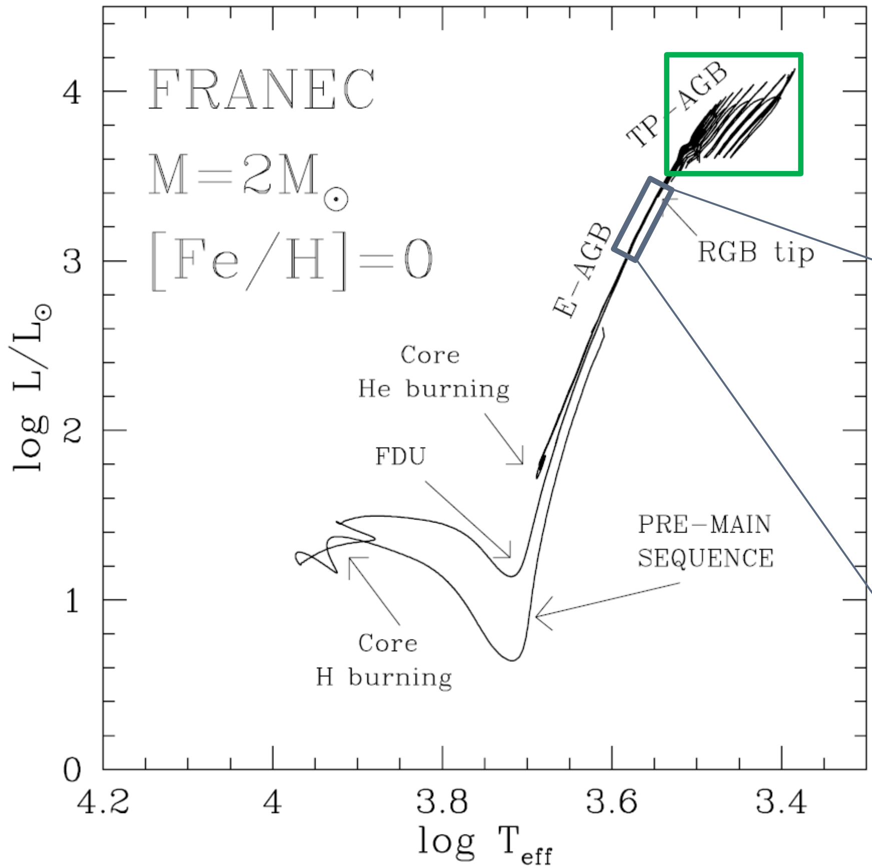

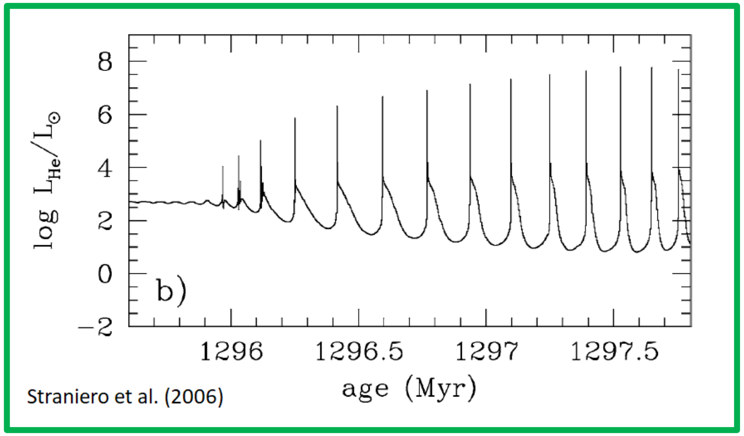

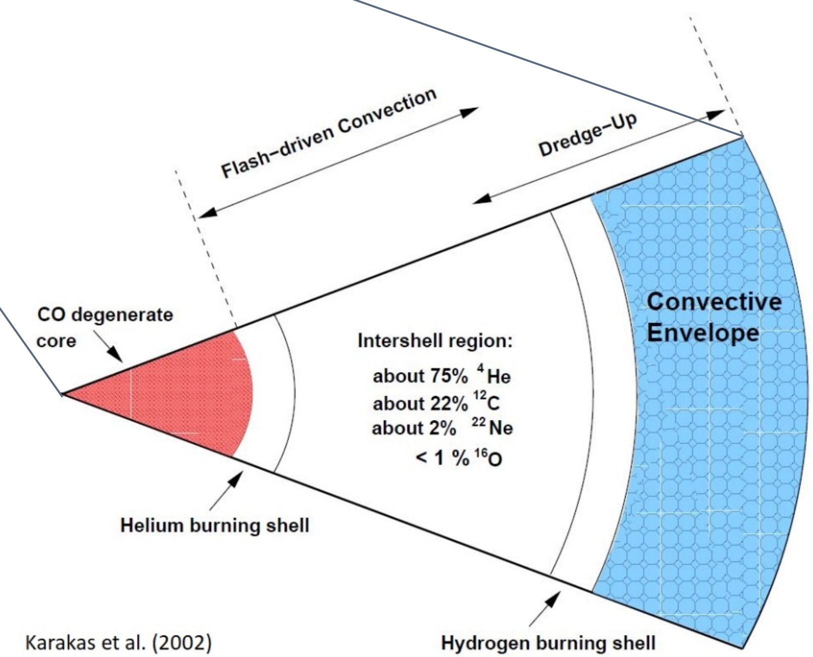

- Low-Mass Stars
- Asymptotic Giant Branch (AGB)
- Thermal Pulses

H- and He-burning in TP-AGB stars

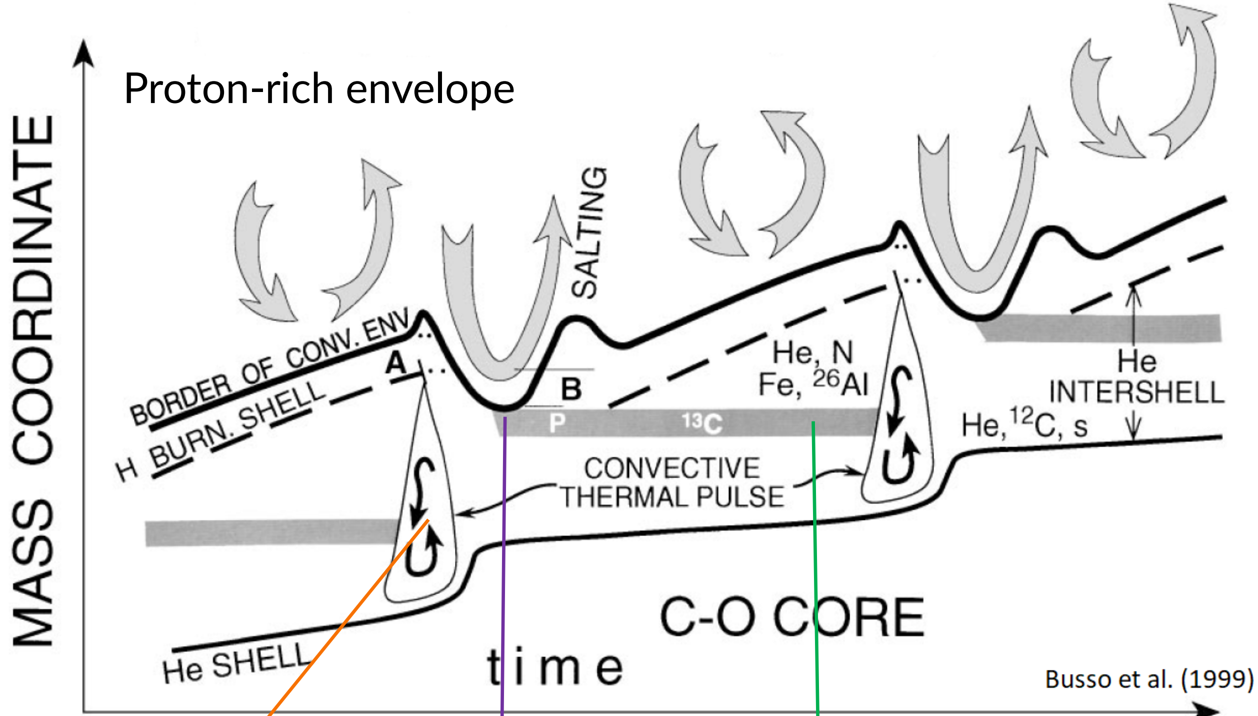

- What?
  Low-Mass Stars
- When?
  Asymptotic Giant Branch (AGB)
- How?
  Thermally Pulsing (TP)

He-flash

proton penetration

^{13}C-pocket

$^{12}C(p,\gamma)^{13}N(\beta^{+}\nu)^{13}C$

$^{22}Ne(\alpha,n)$ — $^{13}C(\alpha,n)$ → heavy elements!!

The ^{13}C-pocket: formation

- **Protons can penetrate** into the He-rich region at each **TDU (Third Dredge-Up) phenomenon**

Which is the physical mechanism?

Classic models **assume** the ^{13}C-pocket formation

Many recent physical approaches:

- Opacity-induced overshoot (Cristallo+ 2009, 2011, 2015)
- Convective Boundary Mixing (Battino+ 2016)
- Magnetic fields (Trippella+ 2016; Palmerini+ 2018)

➡ bottom-up mechanism through
magnetic buoyancy

1) Rotational shears promote magnetic fields
2) Magnetic structures reach the envelope
3) Protons are injested into the He-rich region

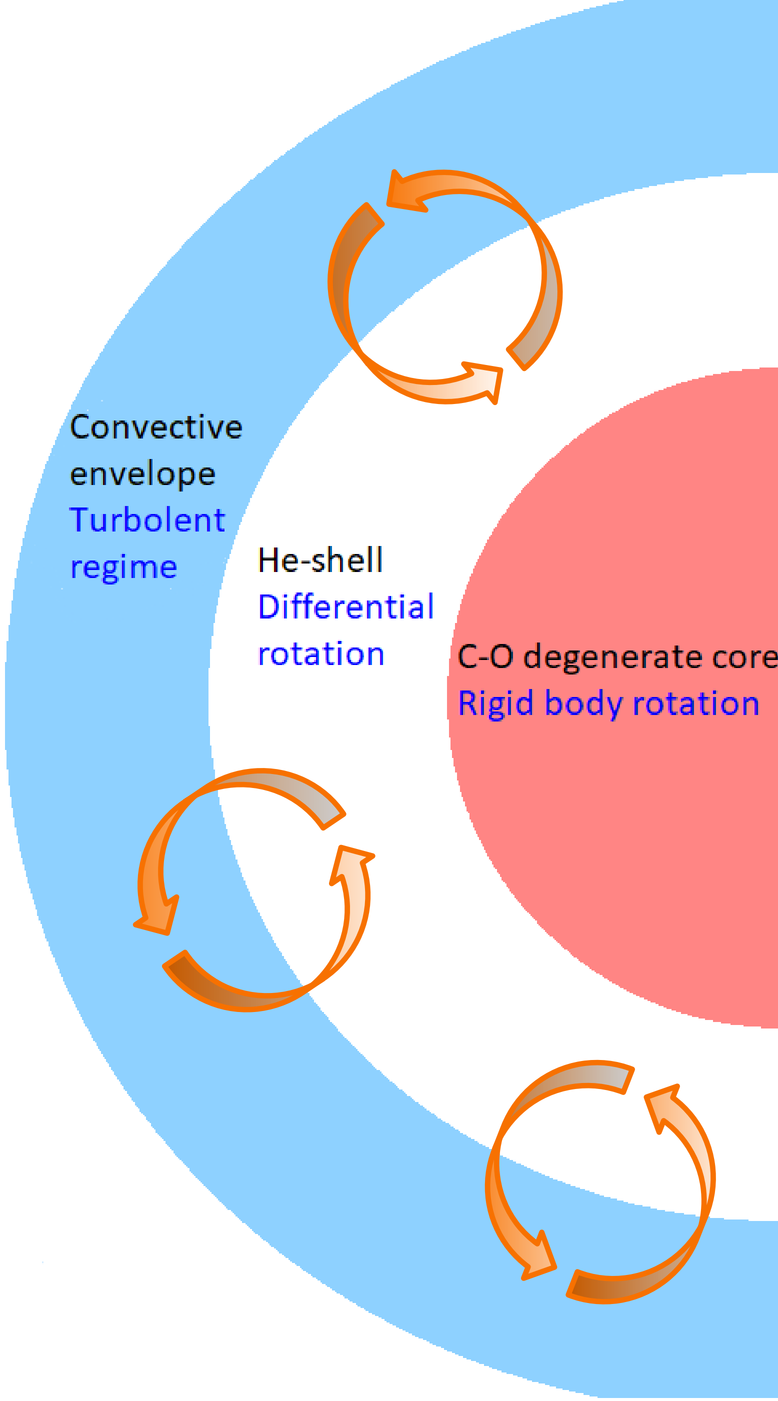

AGB stars and presolar SiC grains

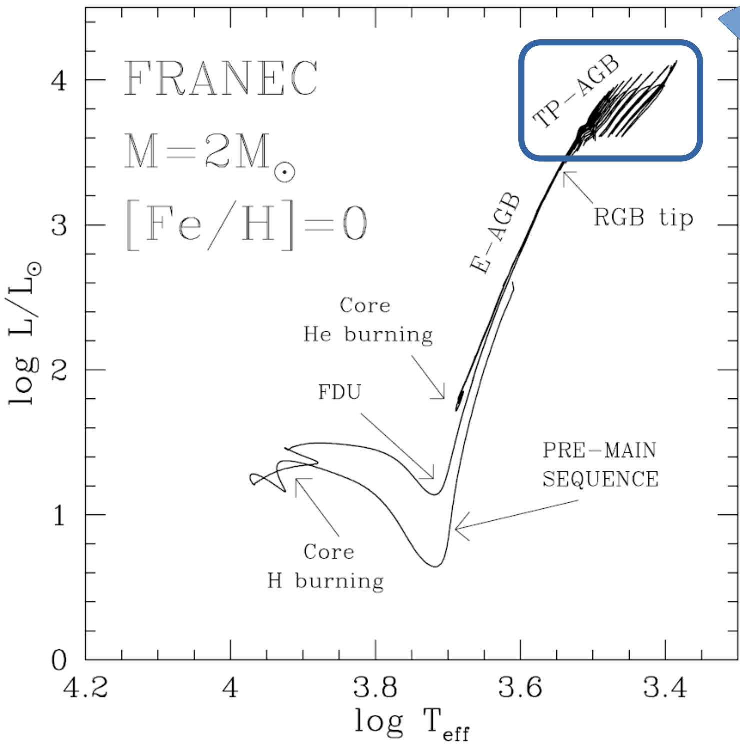

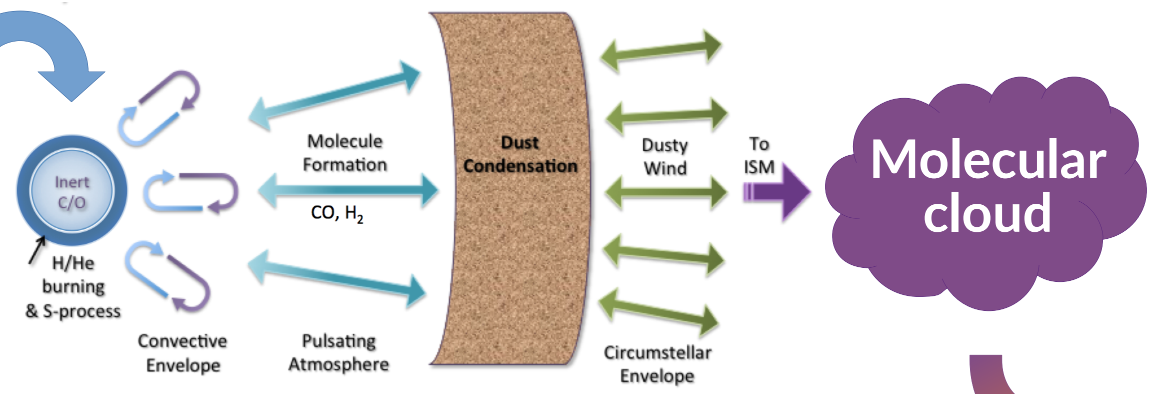

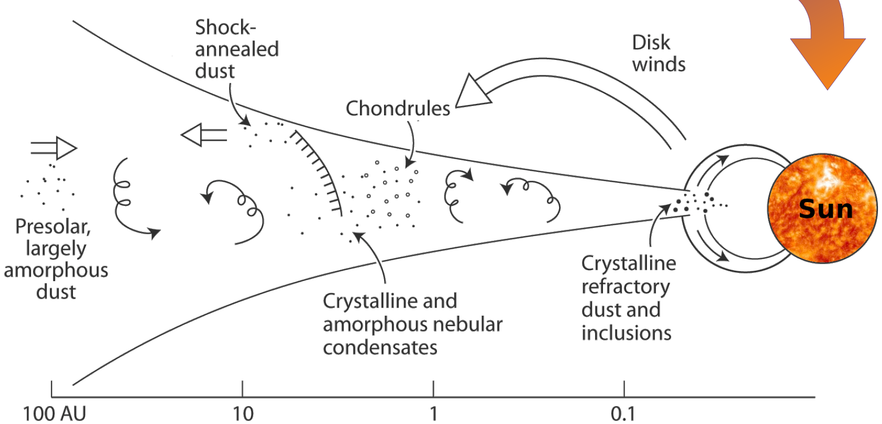

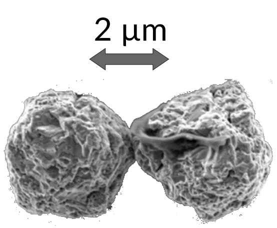

Meteorites and asteroids

Presolar grains

FRUITY models with convective overshooting

- We considered **convective overshooting <u>only</u>** to the partial mixing of hydrogen.

- **Exponential decay** of the convective velocity → $\boxed{v = v_{\mathrm{CE}} \exp\left(-\frac{\Delta r}{\beta H_P}\right)}$

  (Straniero+ 2006, Cristallo+ 2009)

- We considered **isotopic data** including Ni, Sr, Zr, Mo and Ba isotope ratios in **presolar SiC grains →** <u>10% uncertainty</u>

- **One stellar model**: 2 $M_\odot$ and $Z = Z_\odot$

- **Updated** solar-scaled mixture, mass-loss, EOS, nuclear reaction rates

- **Different** values of β

SiC Grains I

- **Isotopic data** including Ni, Sr, Zr, Mo, and Ba isotope ratios in **presolar SiC grains**
- Stellar models with **same initial mass** (2 $M_\odot$) and **solar metallicity**

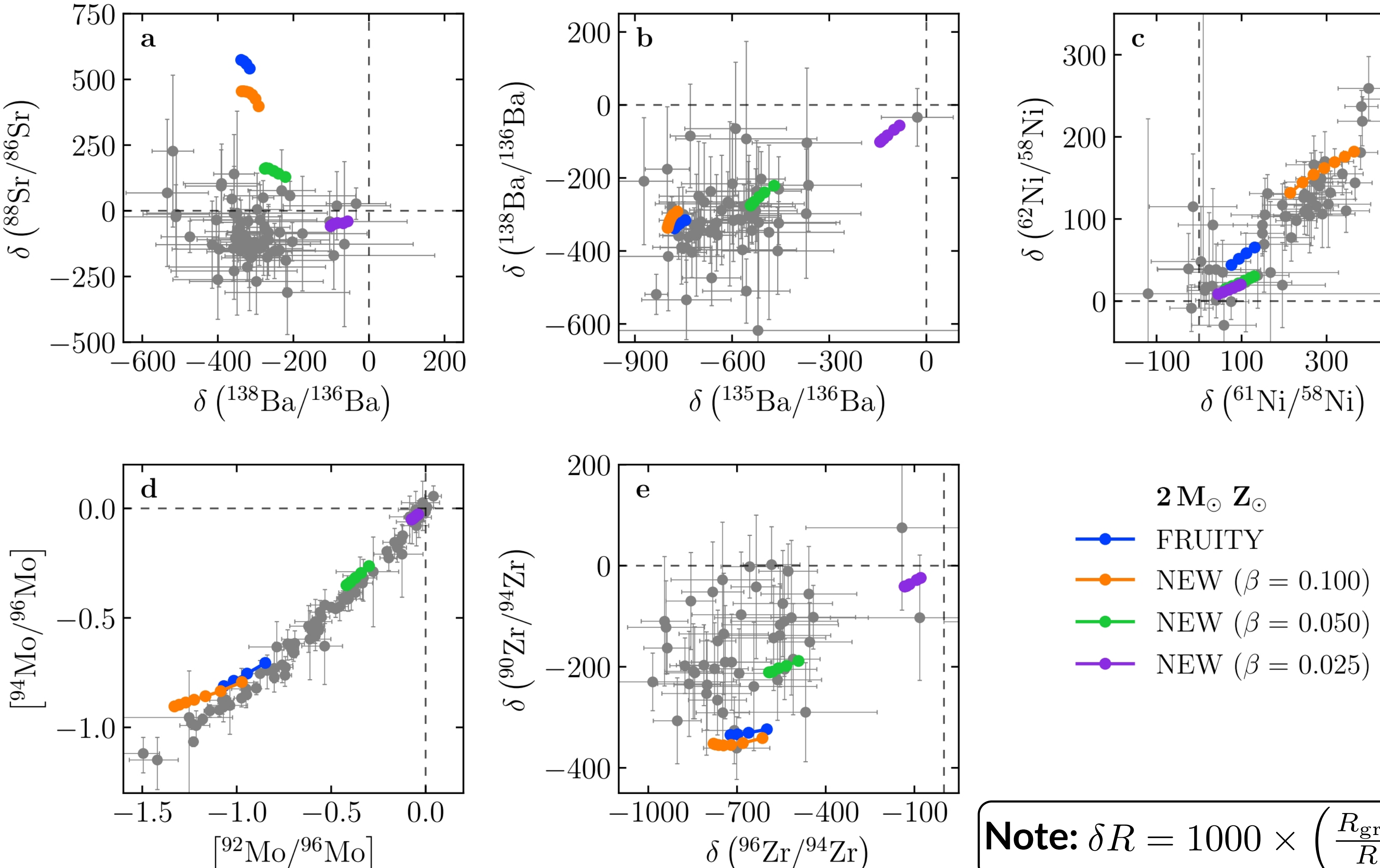

Note: $\delta R = 1000 \times \left(\frac{R_{\mathrm{grain}}}{R_\odot} - 1\right)$

Magnetic buoyancy

- MagnetoHydroDynamics (**MHD**) solutions (Nucci & Busso 2014):
  - No numerical approximations (exact analytic solution)
  - Simple geometry: toroidal magnetic field

Equations:

$$\frac{\partial \rho}{\partial t} + \nabla \cdot (\rho \mathbf{v}) = 0$$

$$\frac{\partial \mathbf{B}}{\partial t} - \nabla \times (\mathbf{v} \times \mathbf{B}) - \nu_m \Delta \mathbf{B} = 0$$

$$\rho \left[\frac{\partial \mathbf{v}}{\partial t} + (\mathbf{v} \cdot \nabla)\mathbf{v} - c_d \mathbf{v} + \nabla \Psi \right] - \mu \Delta \mathbf{v} + \nabla P + \frac{1}{4\pi} \mathbf{B} \times (\nabla \times \mathbf{B}) = 0$$

$$\rho \left[\frac{\partial \epsilon}{\partial t} + (\mathbf{v} \cdot \nabla)\epsilon \right] + P \nabla \cdot \mathbf{v} - \nabla \cdot (\kappa \nabla T) + \frac{\nu_m}{4\pi} (\nabla \times \mathbf{B})^2 = 0$$

Solutions: $$v_r = v_p \left(\frac{r_p}{r} \right)^{k+1} \qquad B_\varphi = B_{\varphi,p} \left(\frac{r}{r_p} \right)^{k+1}$$

where *k* is the exponent of the density distribution: $$\rho(r) = \frac{\rho_p}{r_p^k} r^k$$

Magnetic-buoyancy-induced mixing

- **Magnetic** contribution (Vescovi+ 2020) to the dowflow velocity $\mathbf{v}_d$, acting when the density distribution is $\rho \propto r^k$:

$$v_d(r) = u_\mathrm{p} \left(\frac{r_\mathrm{p}}{r}\right)^{k+2}$$

Parameters:

- Layer "**p**" at the deepest coordinate from which buoyancy starts

  (can be identified from the corresponding **critical toroidal** B_φ value)

$$B_\varphi \gtrsim \left(4\pi\rho r N^2 H_\mathrm{p} \frac{\eta}{K}\right)^{1/2}$$

- Starting velocity u_p of the buoyant material

- Calibration is needed!

- We ran various tests with different parameter values:
  - u_p = 1, 3, 5, 8, 12 × 10^{-5} cm/s
  - B_φ = 2, 5, 10, 15 × 10^4 G

Critical toroidal B-field

- Stellar model: $2\ M_\odot$ $Z = Z_\odot$

- **The critical B_φ** necessary for the onset of magnetic buoyancy instabilities, in radiative zone below the convective envelope **varies from ~10^4 G to ~10^6 G**

- Different values of B_φ correspond to different values of r_p

→ The strength of B_φ **determines the extension** of the mixed zone and, in turn, **of the ^{13}C-pocket**

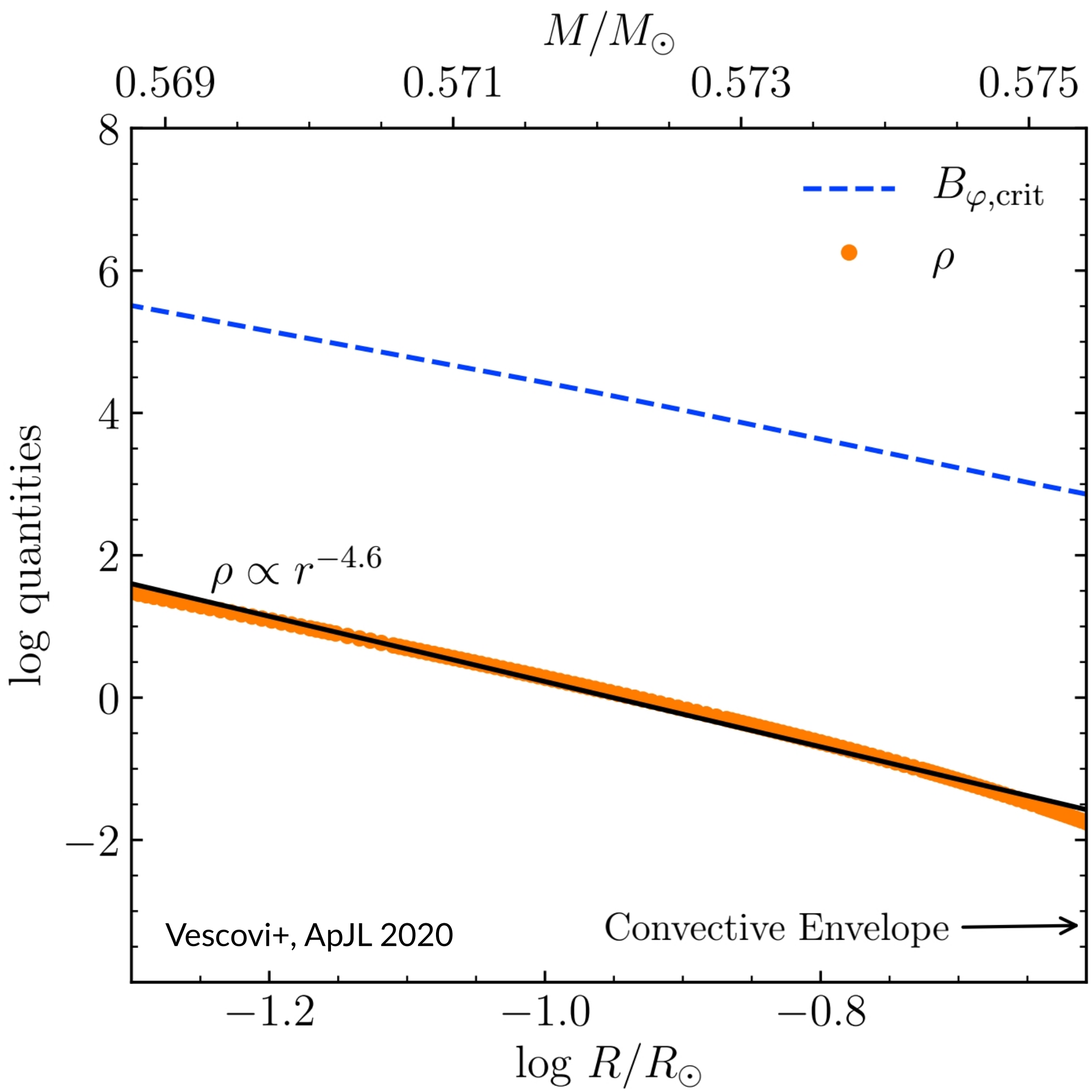

SiC Grains II

- **Magnetic** contribution accounts for SiC data!!
- Best fit for u_p = 5 × 10^{-5} cm/s and B_φ = 5 × 10^4 G

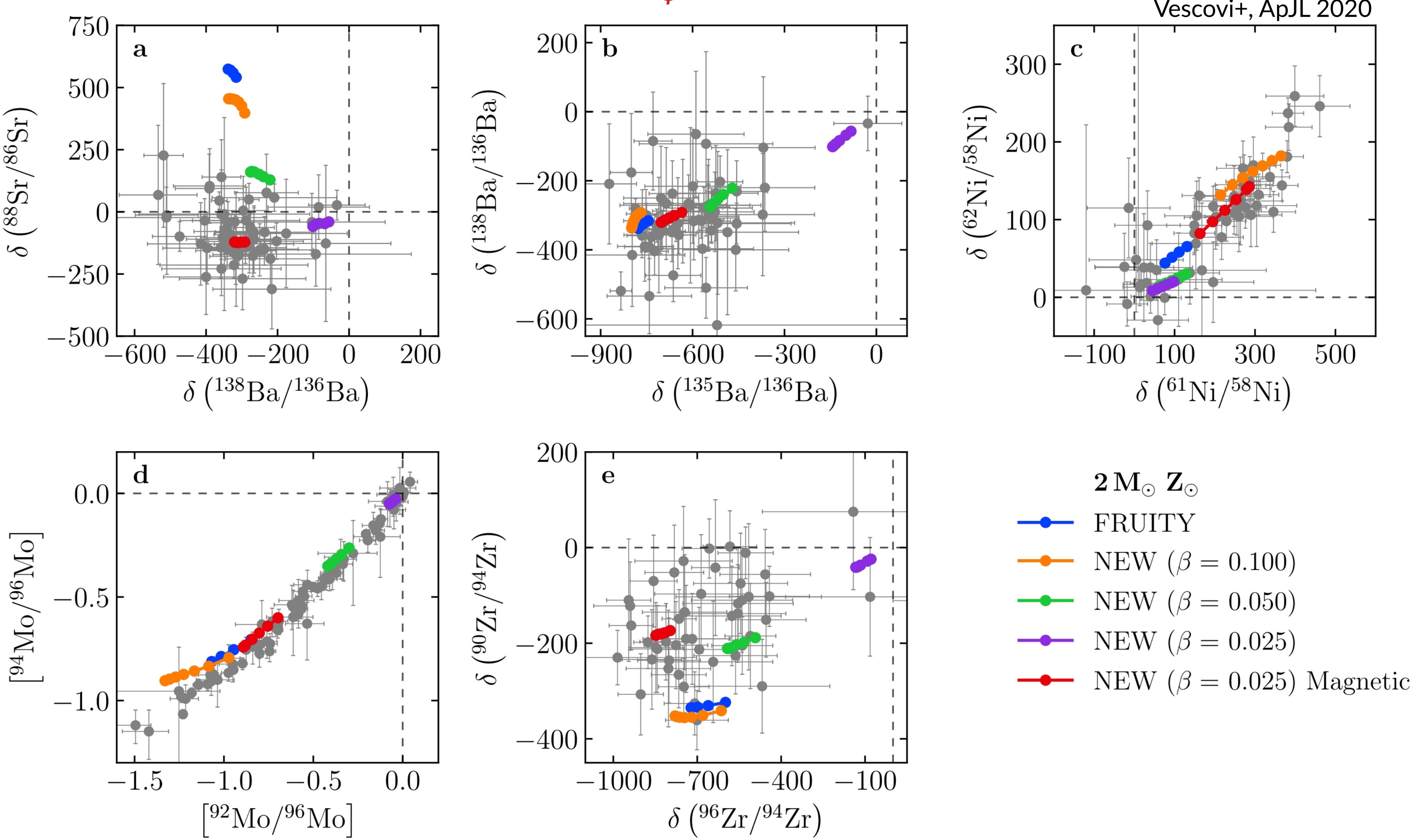

The ^{13}C-pocket: shape

- Effective ^{13}C in the ^{13}C-pocket region –> i.e. the difference between the number fractions of ^{13}C and ^{14}N in the pocket

- New "Magnetic" pocket presents are **more extended and flatter**

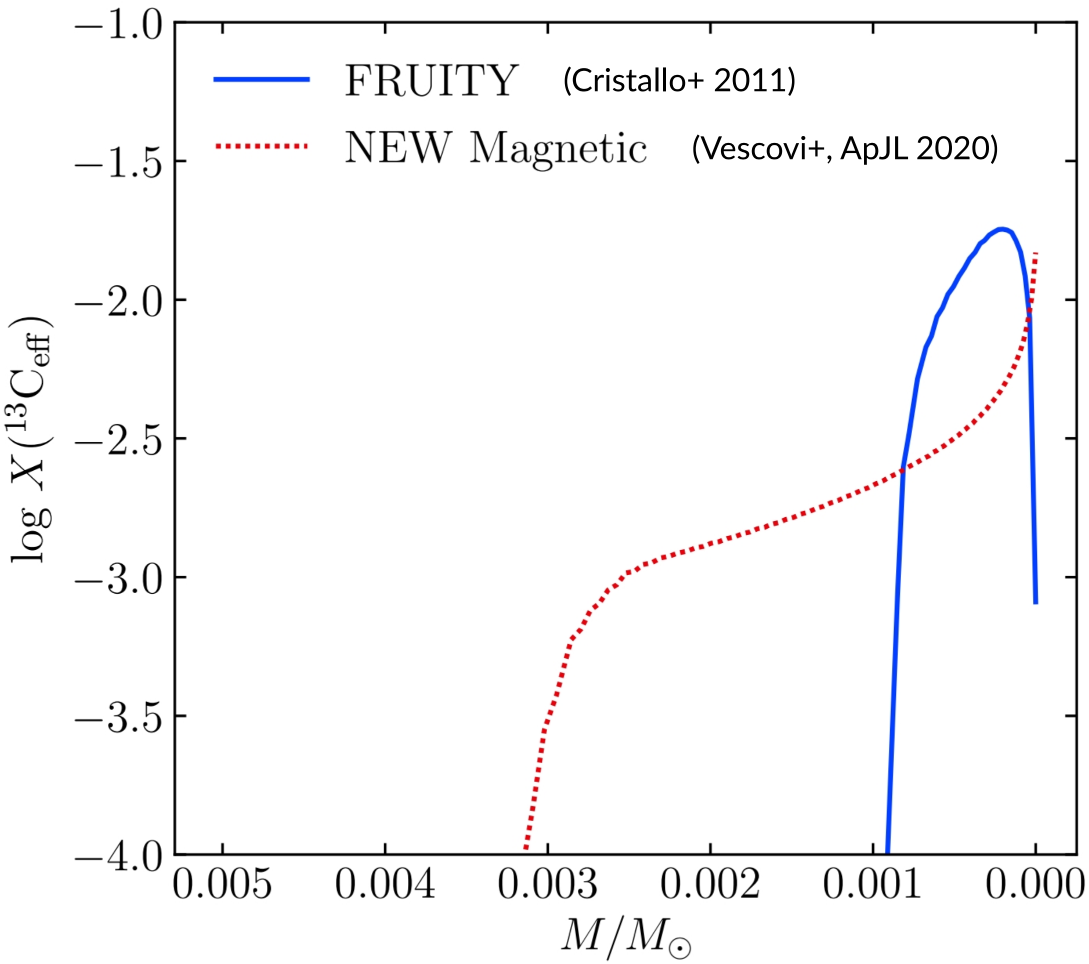

SiC Grains III

- Stellar models with **same initial mass** (2 $M_\odot$) and **close-to-solar metallicity**
- **Magnetic** contribution

Vescovi+, ApJL 2020

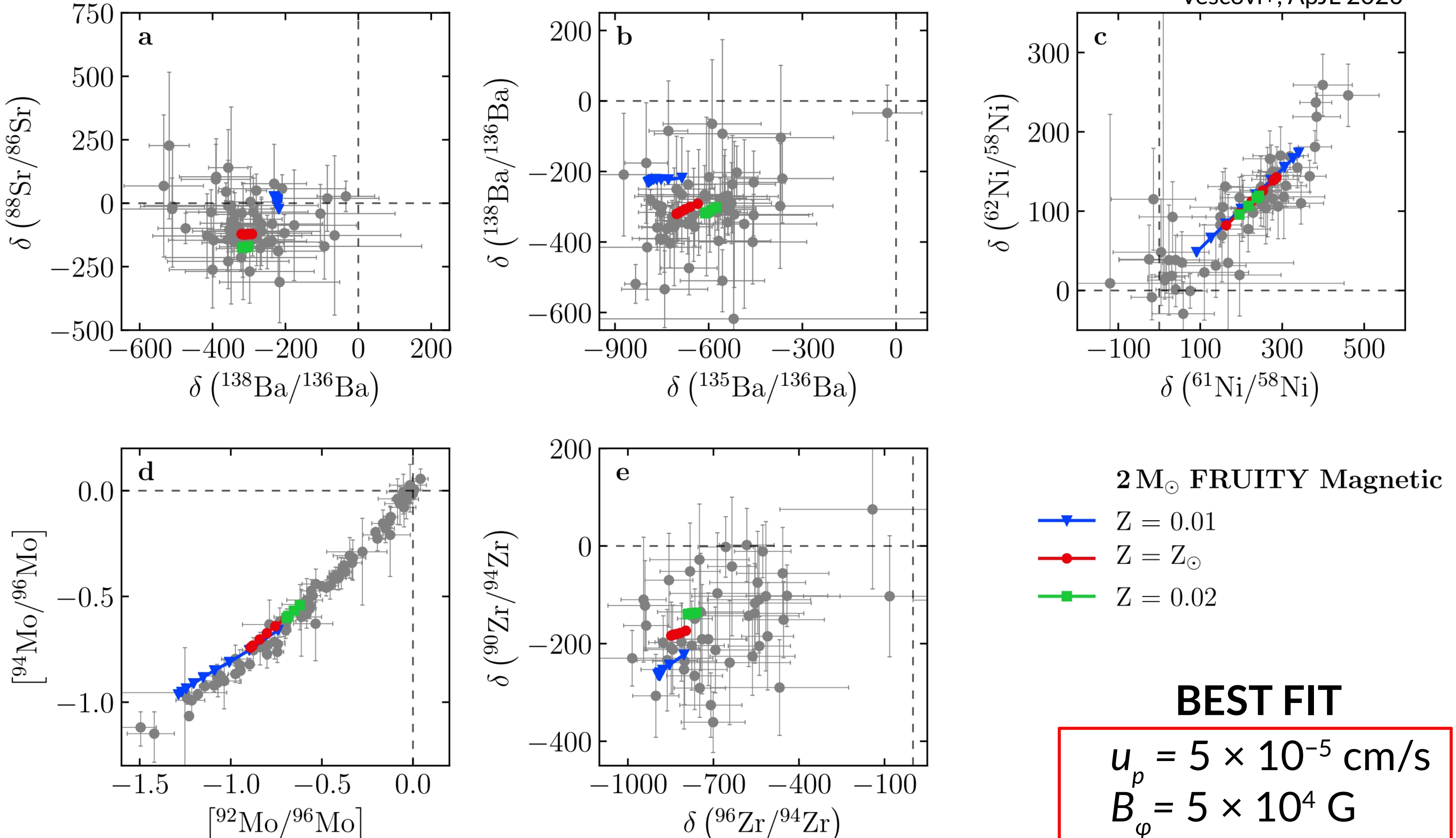

BEST FIT

$u_p = 5 \times 10^{-5}$ cm/s
$B_\varphi = 5 \times 10^{4}$ G

Summary II

- **First numerical simulations** of the formation of a magnetically induced ^{13}C-pocket in a stellar evolutionary code with fully coupled nucleosynthesis

- **Magnetic fields of the order of 10^5 G** (like in the solar tachocline) can induce the formation and buoyant rise of magnetic flux tubes in the He-intershell of AGB stars.

- Such tubes are fast enough to guarantee, by mass conservation, the downward penetration of sufficient protons to form a sizable ^{13}C-pocket

- **Unique choice** of the field strength and initial buoyant velocity

- New magnetic models provide a consistent explanation to the **majority of the heavy-element isotope data** detected in presolar SiC grains from AGB stars

Kilonovae and production of very light elements in Neutron Star Mergers

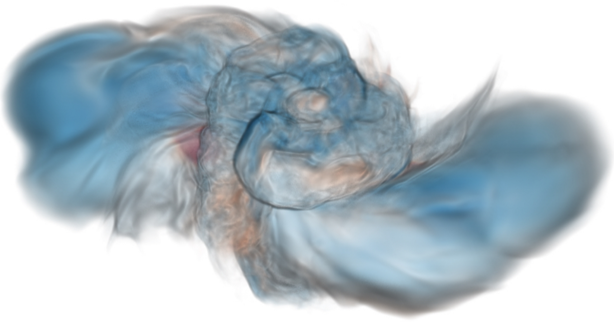

r-process: basic ideas

- key reactions: $(A, Z) + n \leftrightarrow (A + 1, Z) + \gamma$
- *r*-process requires initial high n_n and T
  - → high n_n : $\tau_{(n,\gamma)} << \tau_{\beta\text{-decay}}$
- equilibrium freeze-out: n_n drops and β-decays take over

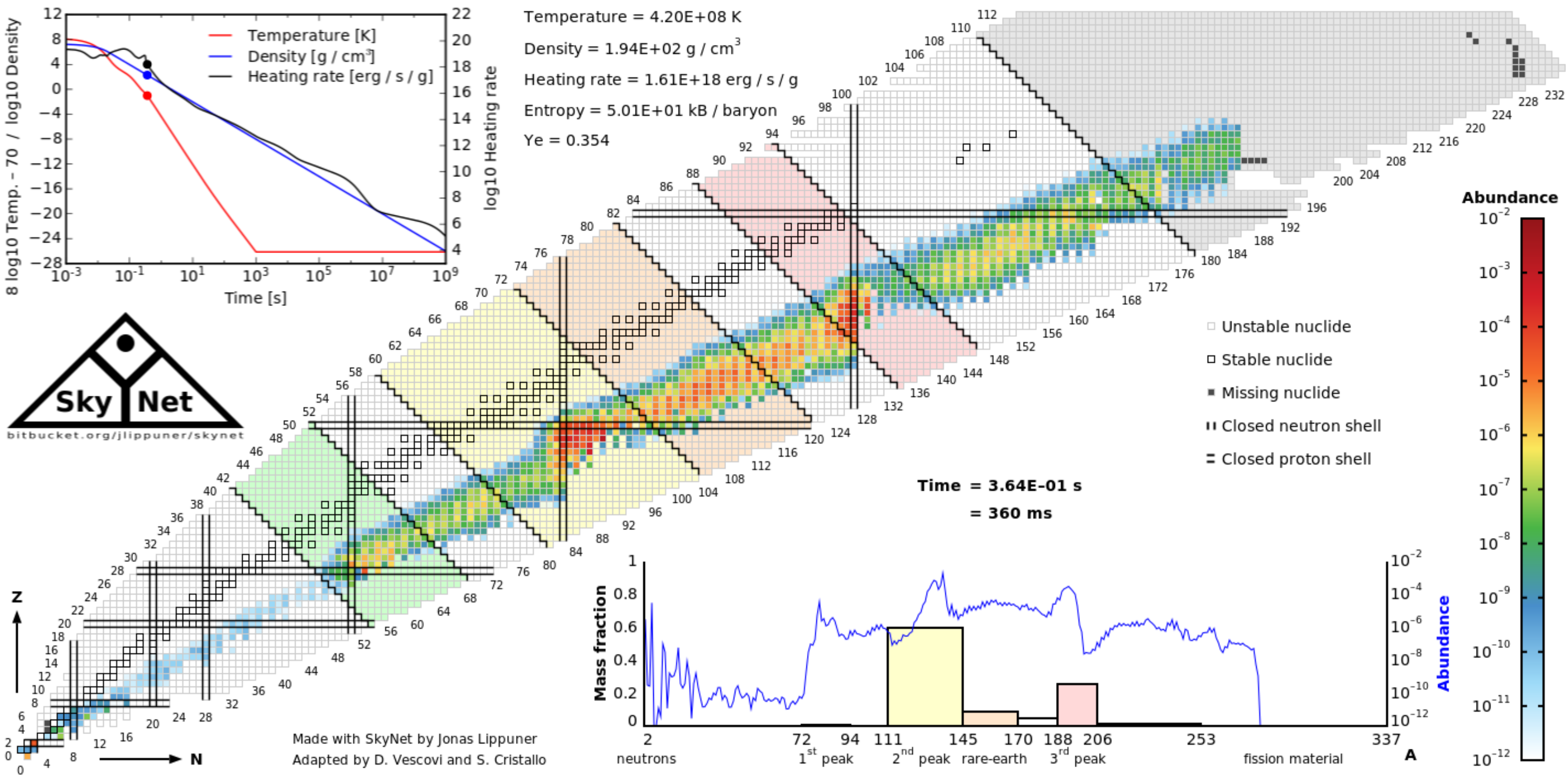

Neutron star mergers as *r*-process site

r-process nucleosynthesis in depends mainly on three physical quantities:

1) entropy $s \sim T^3/\rho$

2) Electron fraction $Y_e \sim n_p/(n_n+n_p)$

3) Dynamical expansion timescale τ_{dyn}

Possible scenarios	high entropy *r*-process	low entropy *r*-process
	hot CCSN winds	BNS and BHNS mergers MHD supernovae

First evidences of *r*-process nucleosynthesis in kilonova from GW170817

r-process nucleosynthesis in BNS mergers

Y_e dominant parameter

- Y_e < 0.15: <u>robust</u> *r*-process, due to several <u>fission cycles</u>
- $Y_e \lesssim 0.25$: 2nd and 3rd *r*-process peaks, but no first
- $Y_e \gtrsim 0.25$: up to 2nd *r*-process peak

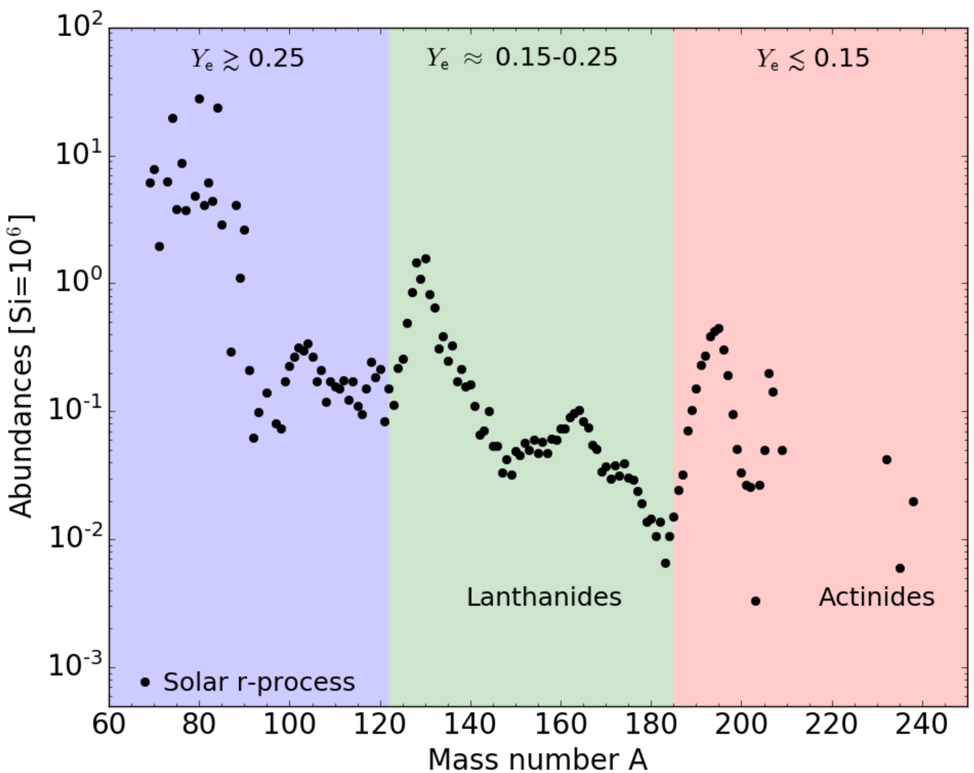

Production of lanthanides dramatically changes photon opacity κ_γ

- no lanthanides:
  low opacity ($\kappa_\gamma \lesssim 1$ cm^2/g)
- presence of lanthanides:
  increased opacity ($\kappa_\gamma \gtrsim 10$ cm^2/g)

BNS merger + kilonova

- Red emission:
  - Tidal ejecta
  - Peak luminosity at days - 1 week after the merger
  - Lanthanide dominated – low Y_e

- Blue emission:
  - Polar ejecta
  - Peak luminosity at 1-2 days after the merger
  - 1st/2nd peak dominated – high Y_e

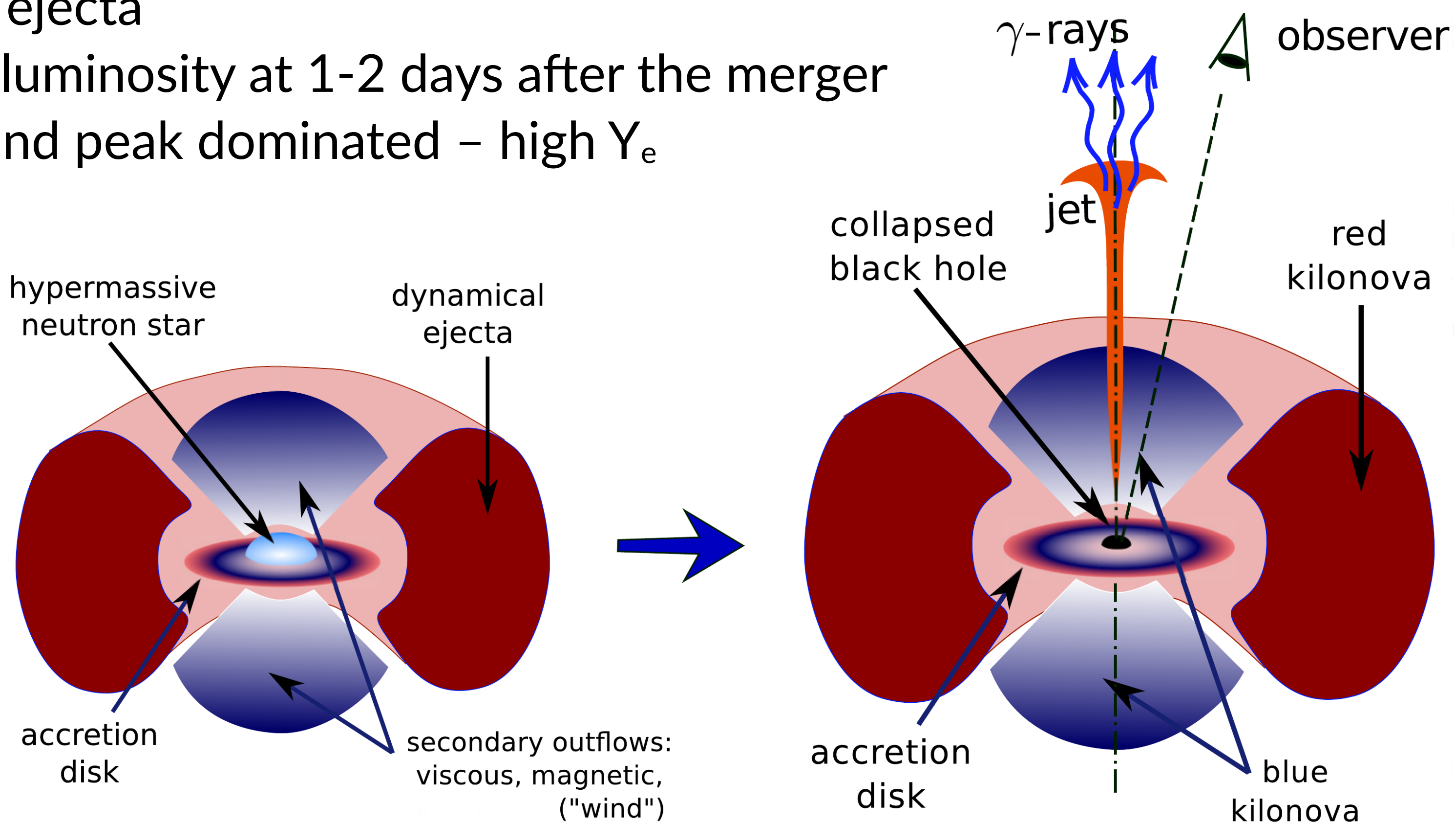

Courtesy of O. Korobkin

Properties of GW170817/AT2017gfo

- 17/08/17, GW+EM detection of an event compatible with BNS merger (LVC PRL 2017)
- Blue component
- Red component
- Thermal emission by radiocative decay of heavy elements synthesized in multicomponent (2-3) ejecta

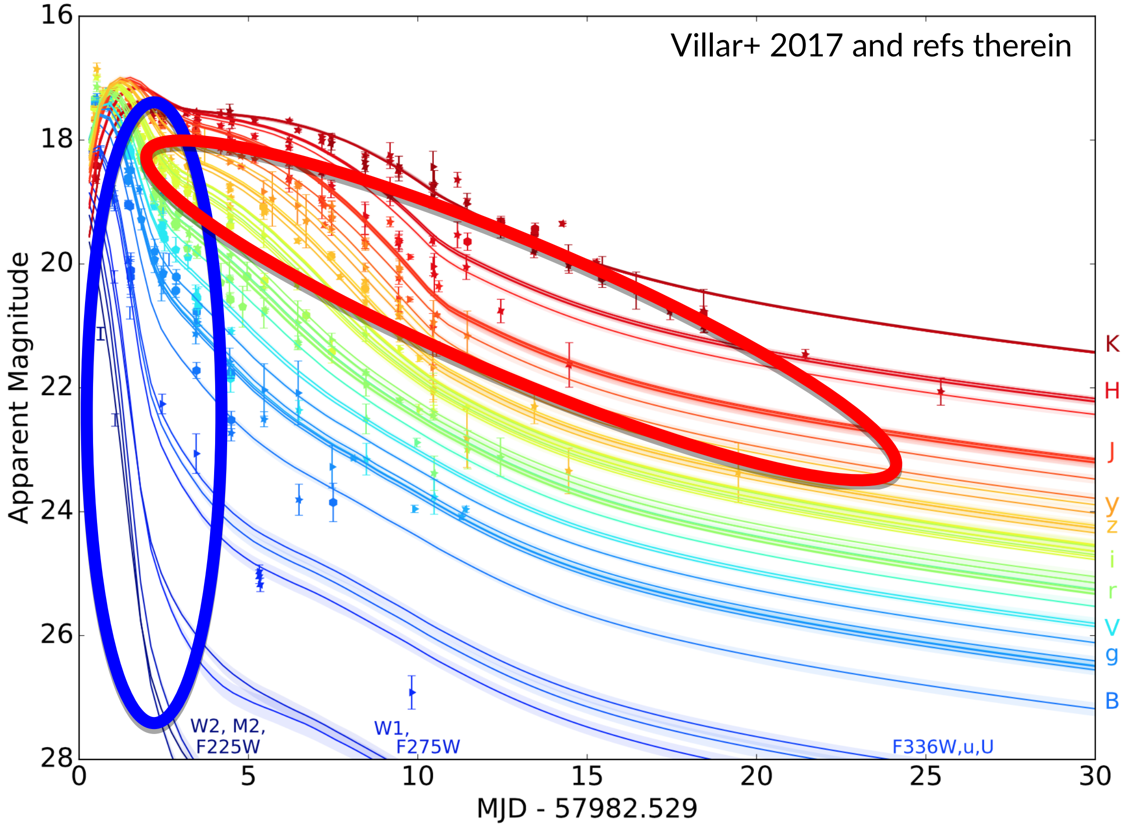

Properties of GW170817/AT2017gfo

Spectral analysis hampered due to:

- Heavy elements have **forest of lines** hence strong blending
- **Relativistic velocity** makes for extremely broad lines (multi-components and different velocities)
- Atomic data are incomplete and uncertain

➔ The analysis of the spectrum at 1.5 days suggested the presence of **strontium** (Watson +2019)

Watson+ 2019

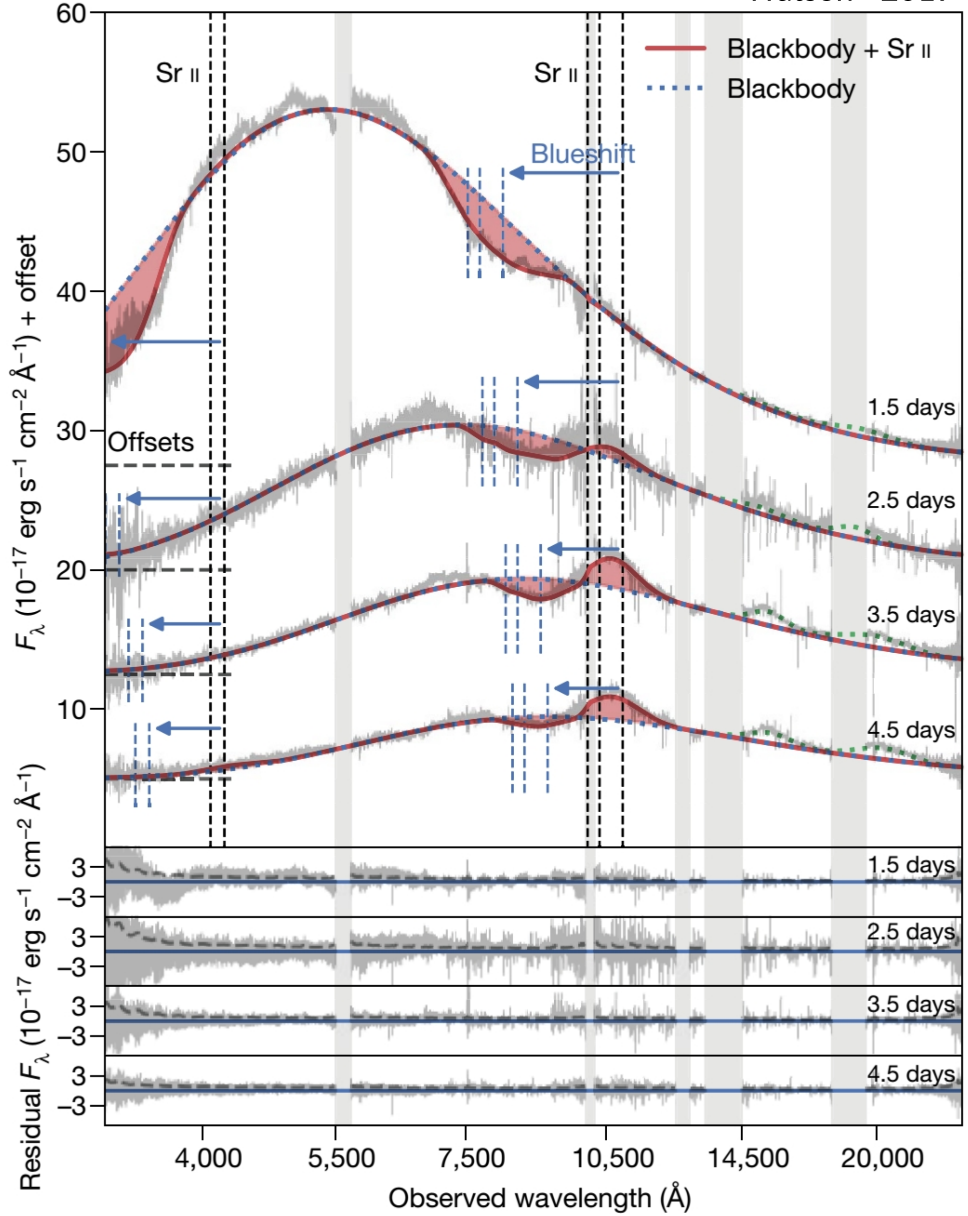

Production of very light elements in kilonovae

- What about very light elements?

- The dynamical ejecta and spiral-wave wind are the earliest and fastest ejecta

  → transparent within the very first days and possibly providing key spectral features

- we investigated the production of <u>light elements</u> ($Z < 20$)

- connecting the thermodynamics conditions for their production to the binary properties (mass ratio and EOS)

- study their early detectability

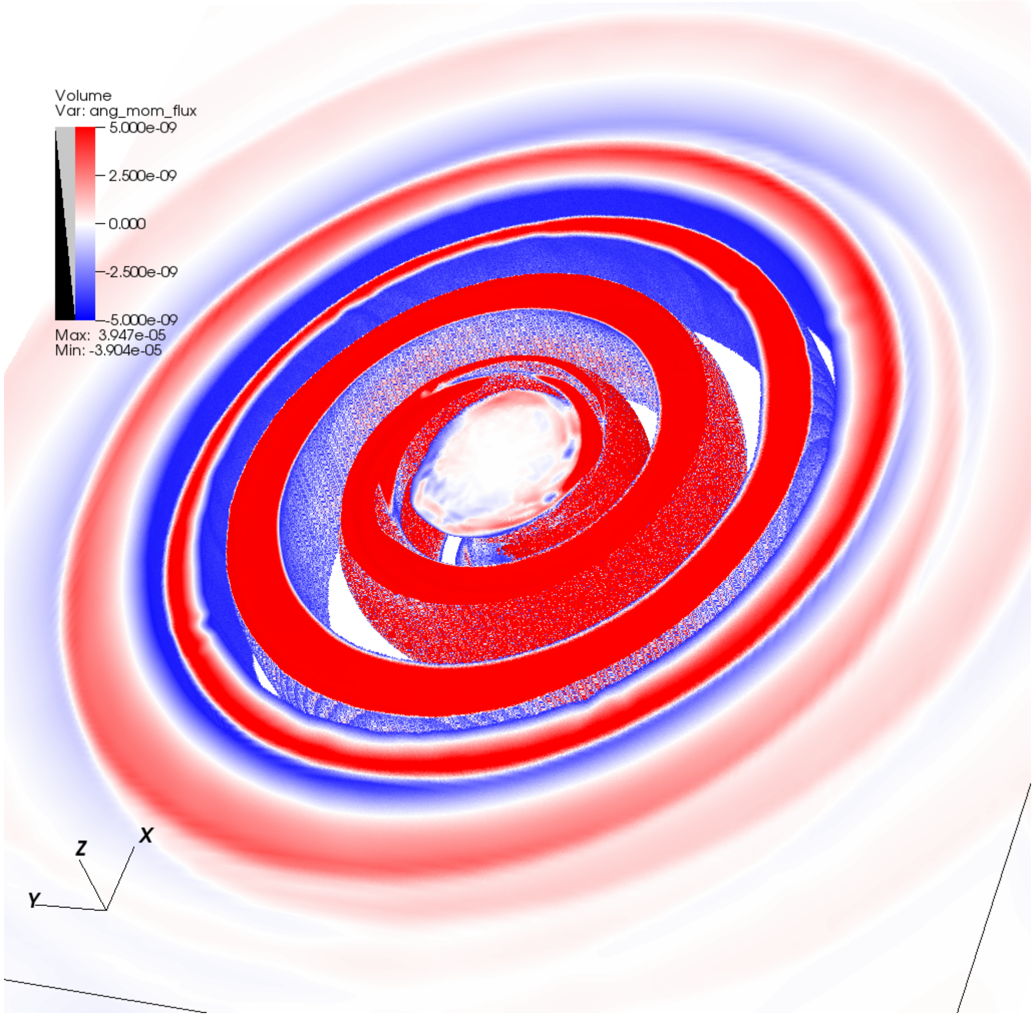

Spiral-wave wind (Nedora+ 2019, 2020)

Production of very light elements in kilonovae

- Three simulations:

  1) $M_1 = M_2 = 1.364\ M_\odot$

  Soft EOS (BLh)

  2) $M_1 = 1.856\ M_\odot$, $M_2 = 1.020\ M_\odot$

  Soft EOS (BLh)

  3) $M_1 = M_2 = 1.364\ M_\odot$

  Stiff EOS (DD2)

- from each BNS simulations we extract mass distributions of the ejecta in the s, Y_e, τ_{dyn} space

- **time-dependent abundances** from their convolution with the yields tabulated with *SkyNet* (Lippuner & Roberts 2017)

Production of very light elements in kilonovae

- **H and He are the most abundant** species, <u>comparable to Sr</u>, lanthanides, and actinides
- **elements between lithium and potassium are** usually several orders of magnitudes **less abundant**

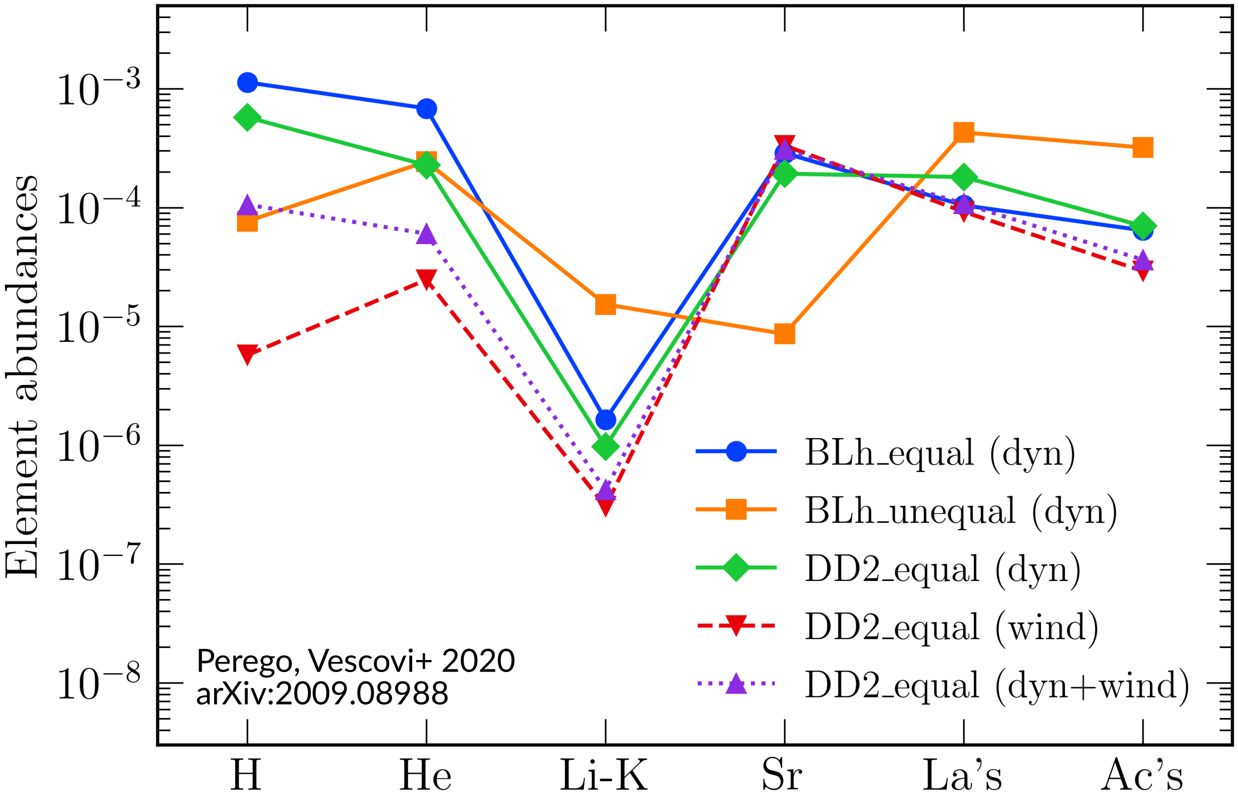

Conditions of the ejecta from BNS merger simulations

- The **bulk** of the ejecta has low entropy (s < 40 k_B baryon^{-1}) and is neutron rich
- Equatorial ejecta are usually characterized by lower Y_e and lower entropy
- However, at both angles a high-entropy **tail** (with s > 60 k_B baryon^{-1}) expanding at high speeds (τ <~ 5 ms) is visible

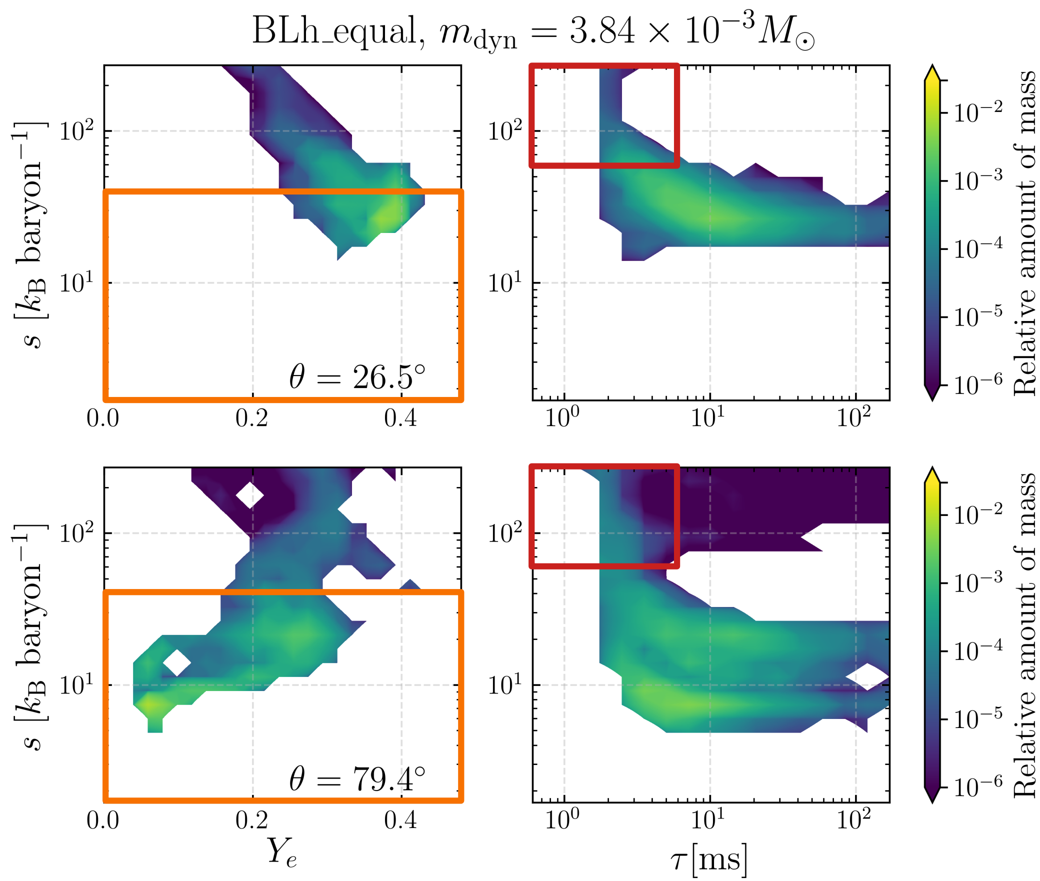

Origin of H, He, and Sr

Abundances at 2 days for $\tau = 1.0$ ms (top) and $\tau = 11.4$ ms (bottom) trajectories

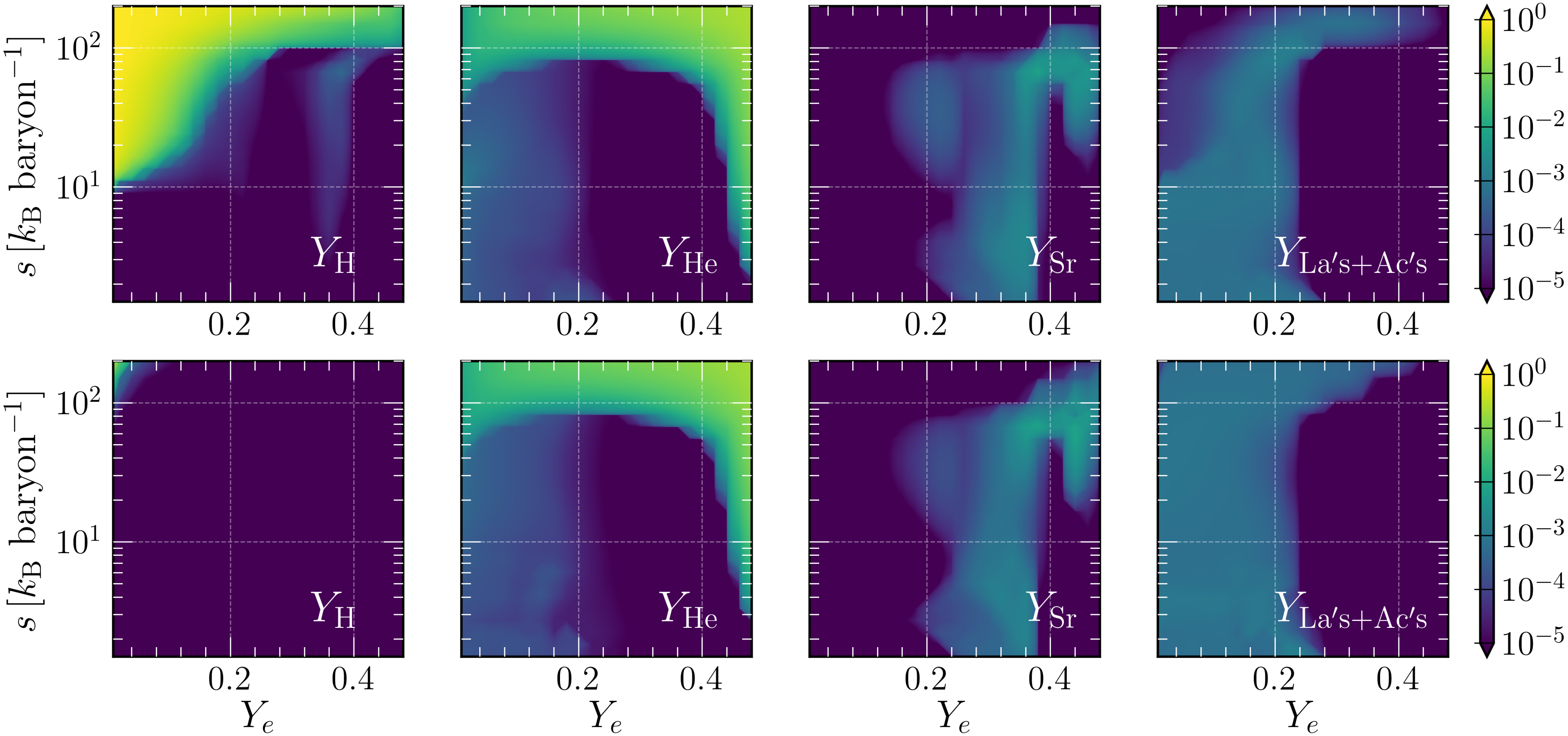

- Abundances for individual trajectories characterized by different (s, Y_e, τ) sets
- For Ye ≳ 0.22 **Sr is robustly produced** for all entropies

Origin of H, He, and Sr

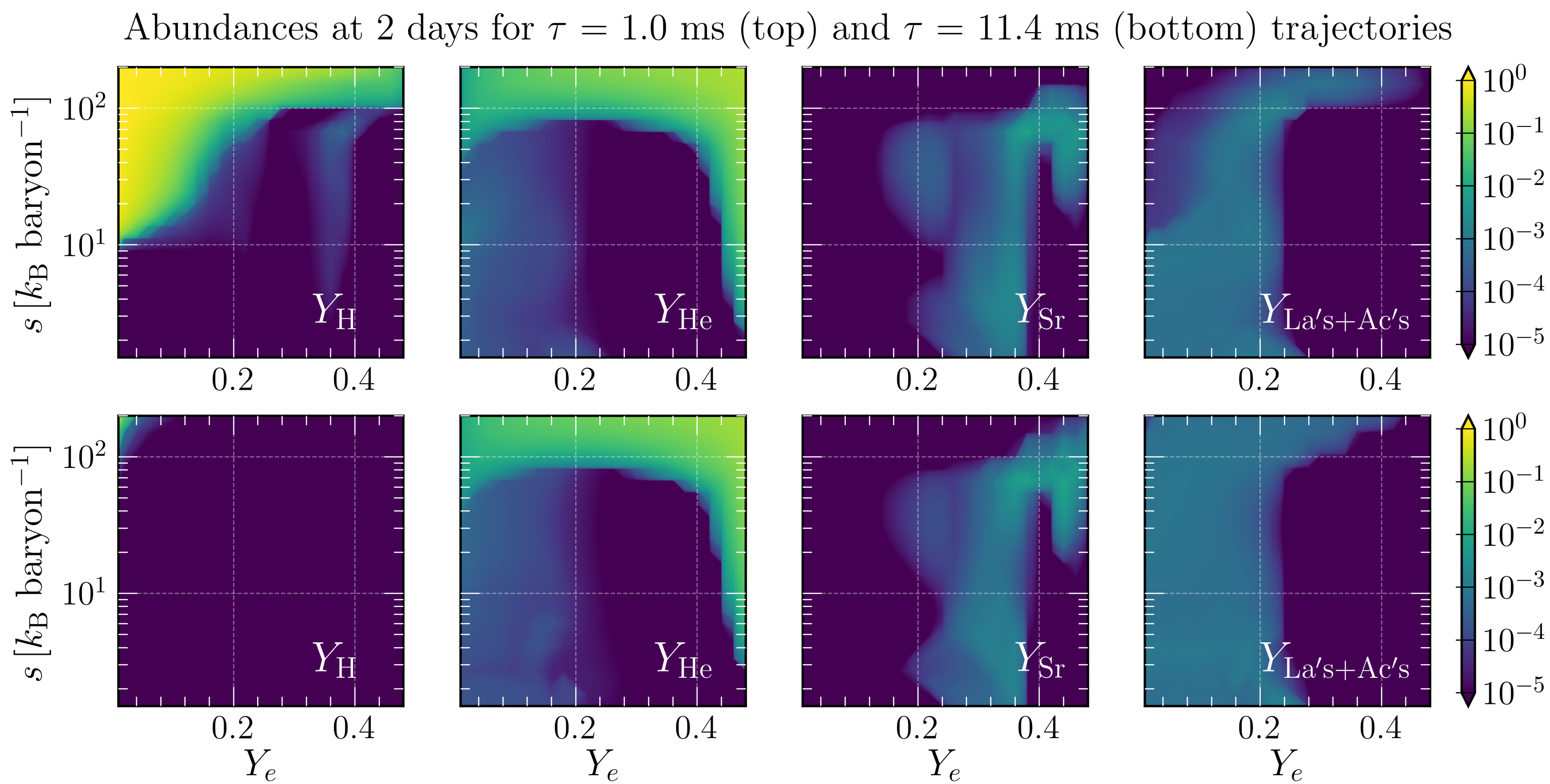

- The presence of **H** in the ejecta is related with **high-*s*** and **low-Y_e**
- He production can happen both in association or in the absence of heavy elements

Detecting H, He, and Sr in kilonova spectra

- The amount of Sr predicted by ab-initio BNS models is **consistent** with the one required by the analysis reported in Watson+ 19
- He and then H could **recombine in** atomic form after a **few hours**
- However, they probably **never contribute** to the kilonova spectrum
- Presence of H/He lines

  → Supernovae

Perego, Vescovi+ 2020
arXiv:2009.08988

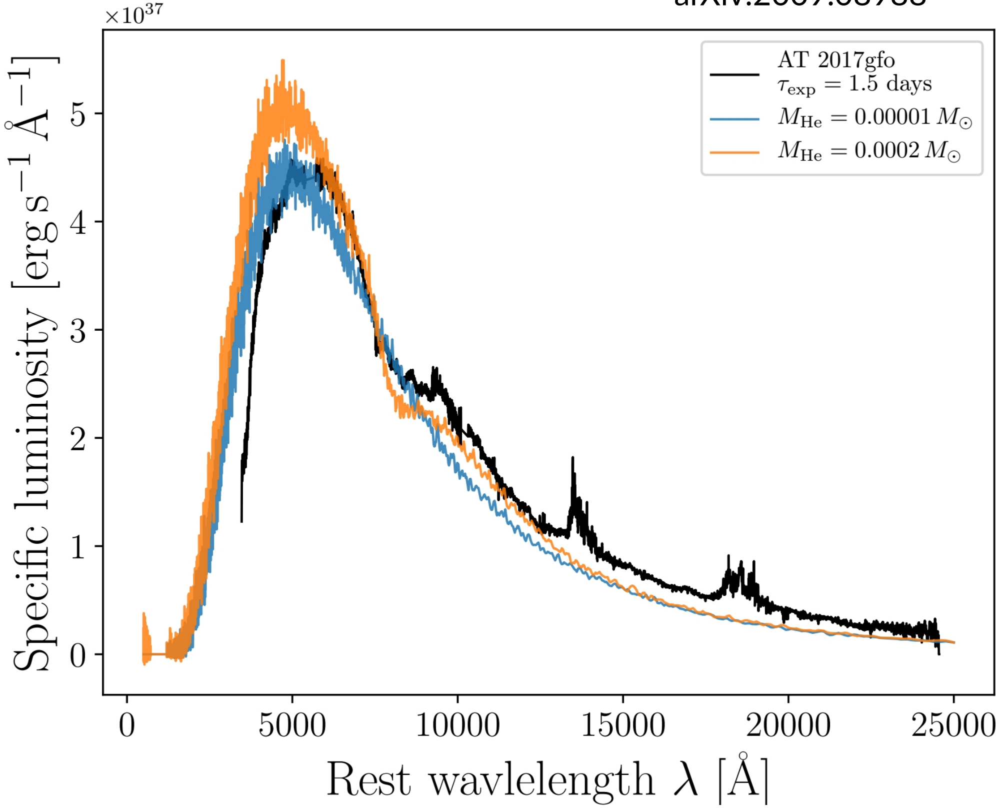

Summary III

- We considered results of Numerical Relativity (NR) simulations of BNS assuming different mass-ratio and EOS

- <u>In BNS mergers H, He, and Sr can be synthesized</u>

- The amount of Sr is **consistent** with the one required to explain early spectral features in the kilonova of GW170817

- H and He probably **never contribute** to the kilonova spectrum formation unless strong non-LTE effects appear or a dramatic EOS softening boosts the presence of fast expanding, high-*s* matter

- Key result to organize and prioritize future observational campaigns for the electromagnetic counterparts of GW events

Backup Slides

Standard Solar Model (SSM)

- Stellar model obtained by numerical integration of the equations describing the physical and chemical structure of the Sun as well as its time evolution

$$\frac{\partial r}{\partial m} = \frac{1}{4\pi r^2 \varrho}$$
$$\frac{\partial P}{\partial m} = -\frac{Gm}{4\pi r^4}$$
$$\frac{\partial l}{\partial m} = \varepsilon_{\rm n} - \varepsilon_{\nu} - \varepsilon_{\rm g}$$
$$\frac{\partial T}{\partial m} = -\frac{GmT}{4\pi r^4 P}\nabla$$

$$\frac{\partial X_i}{\partial t} = \underbrace{\boxed{R_i}}_{\text{Nuclear reactions}} + \underbrace{\boxed{M_i}}_{\text{Mixing (convection)}} + \underbrace{\boxed{DG_i}}_{\text{Diffusion Gravitational settling}}$$

- Evolve a model with 1 $M_\odot$ starting from a chemically homogeneous model to present solar age with:

  1) good microphysics (reaction rates, equation of state (EOS), opacity)

  2) assumed mixing length (<u>α_{ml}</u>), initial helium (<u>Y_{ini}</u>) and metal (<u>Z_{ini}</u>) abundances

→ **Match $R_\odot$, $L_\odot$, and $(Z/X)_\odot$ to better than one part in 10^{-5}**

SSM: predictions

- <u>Physical quantities</u>: temperature, pressure, density, luminosity, mass...

- <u>Chemical profiles</u>: X(r), Y(r), Z_i (r) → electron density profiles

- <u>Helioseismic quantities</u>: surface helium abundance, depth of the convective envelope, sound speed

- <u>Neutrino fluxes</u>: production profiles and integrated values

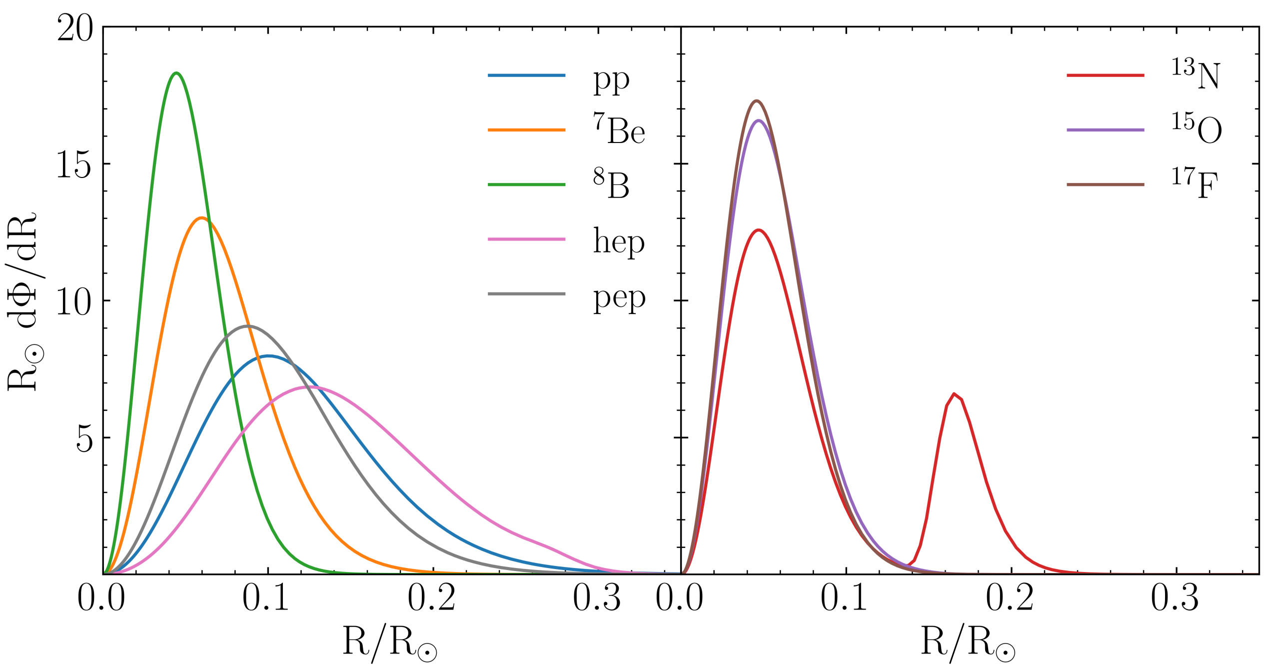

Sun's core metallicity

$$Z_\odot^{\mathrm{c}} = 0.400 \times \frac{\Phi_{\mathrm{CNO}}}{10^{10}\mathrm{cm}^{-2}\mathrm{s}^{-1}}$$ (Gough 19)

$$\Downarrow$$

$$Z_\odot^{\mathrm{c}}\left(\Phi_{\mathrm{CNO}}^{\mathrm{BX}}\right) = 0.028^{+0.012}_{-0.008}$$

Source	Z_{c}
GS98	0.0203 ± 0.0026
PLJ14	0.0179 ± 0.0021

Magnetic field in O-rich and C-rich AGB stars

- Generally, AGB magnetic field measurements come from <u>maser polarization observations</u> (SiO, H2O and OH) (e.g. Vlemmings+ 2012)
- These have revealed a <u>strong magnetic field throughout the circumstellar envelope</u>
- **B-field at surface ~ few G**
- Although the maser observations trace only oxygen-rich AGB stars, recent CN Zeeman splitting observations (Duthu+ 2017) indicate that **similar strength fields are found around C-rich stars**

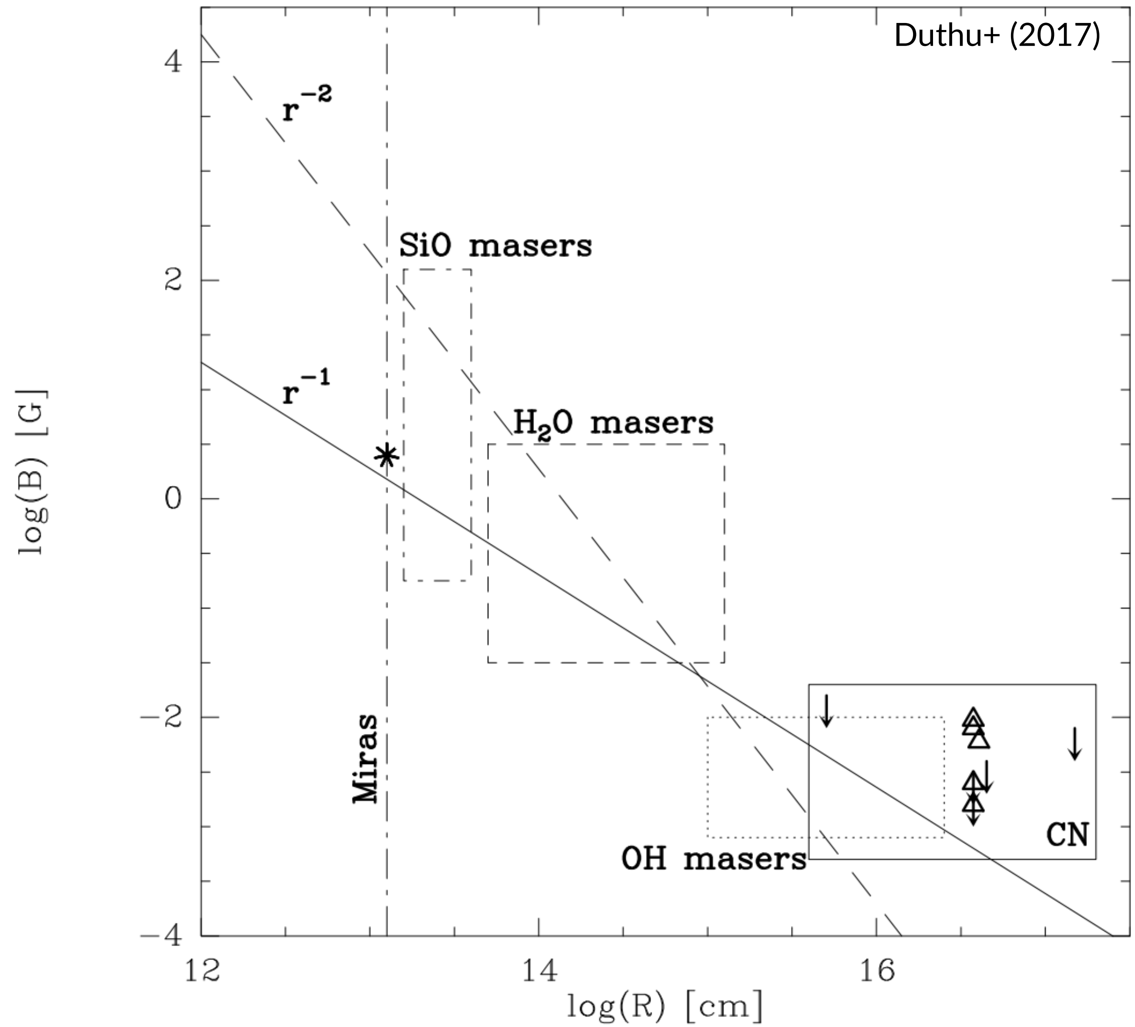

Generation of a toroidal B-field in the He-intershell

- <u>Stellar model</u>: 2.5$M_\odot$ $Z=Z_\odot$
- Stretching of a preexisting **poloidal field** can generate a toroidal field

$$\Rightarrow \frac{\partial B_\varphi}{\partial t} = \frac{1}{r}\frac{\partial}{\partial r}\left(\Omega r^2 B_\mathrm{p}\right) = \Omega q B_\mathrm{p}$$

- <u>Differential rotation</u> in the He-intershell?
- An additional <u>artificial viscosity</u> of around $10^7 \mathrm{cm^2 s^{-1}}$ provides a sufficient transport of angular momentum to match the core and envelope rotation rates for core He-burning stars (den Hartogh + 2019a,b)
- The **critical polidal B_p** would be

$$\Rightarrow B_\mathrm{p} \sim B_\varphi (\Omega q \Delta t)^{-1}$$

- A rough (preliminary) estimate gives a **B_p few hundreds times lower than B_φ** $\Rightarrow$ **$B_p \lesssim 1$kG**

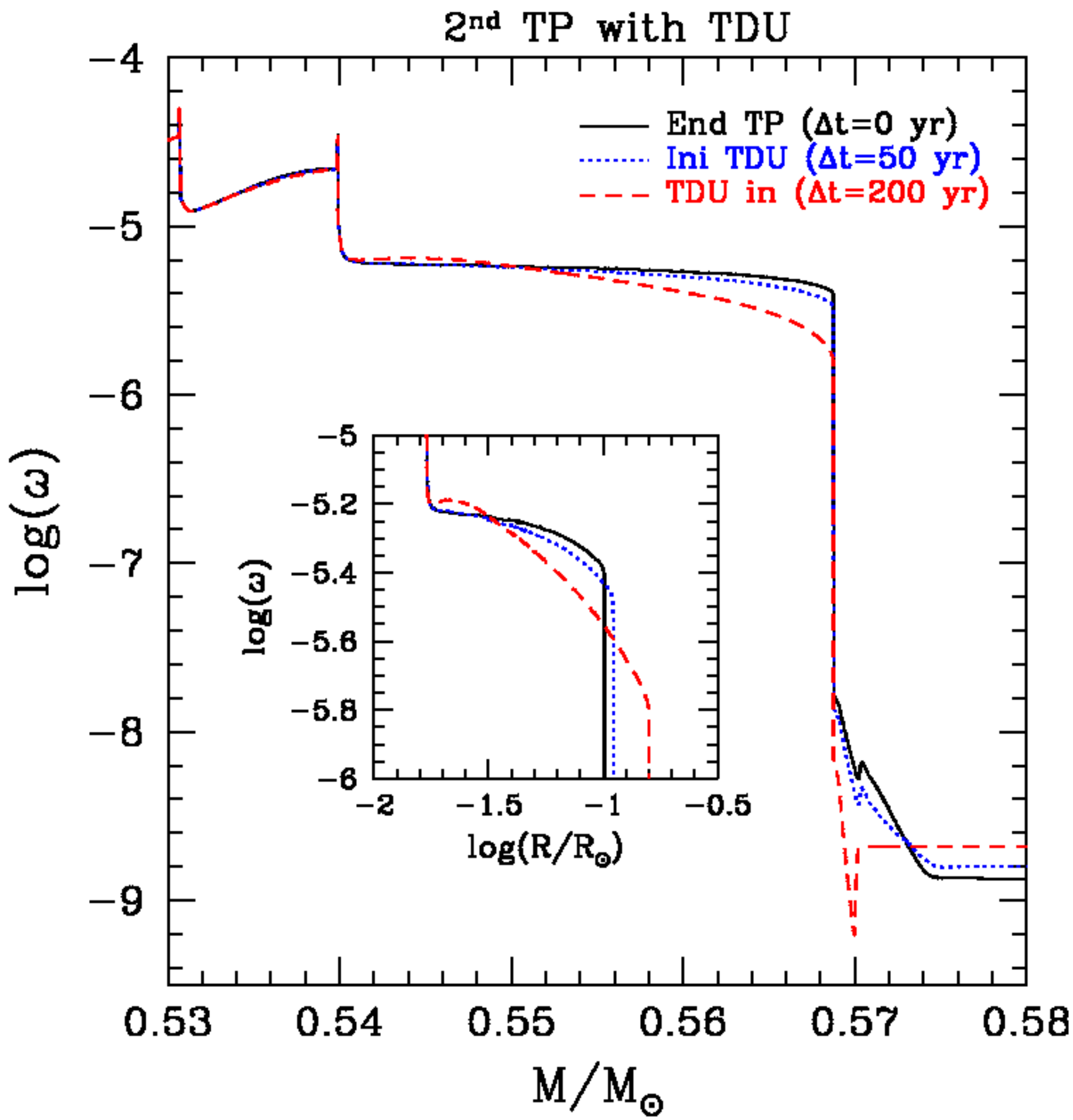

Not implausible!!

Final abundances vs. electron fraction Y_e

- **Threshold value $Y_{e,crit}$ ≈ 0.25**

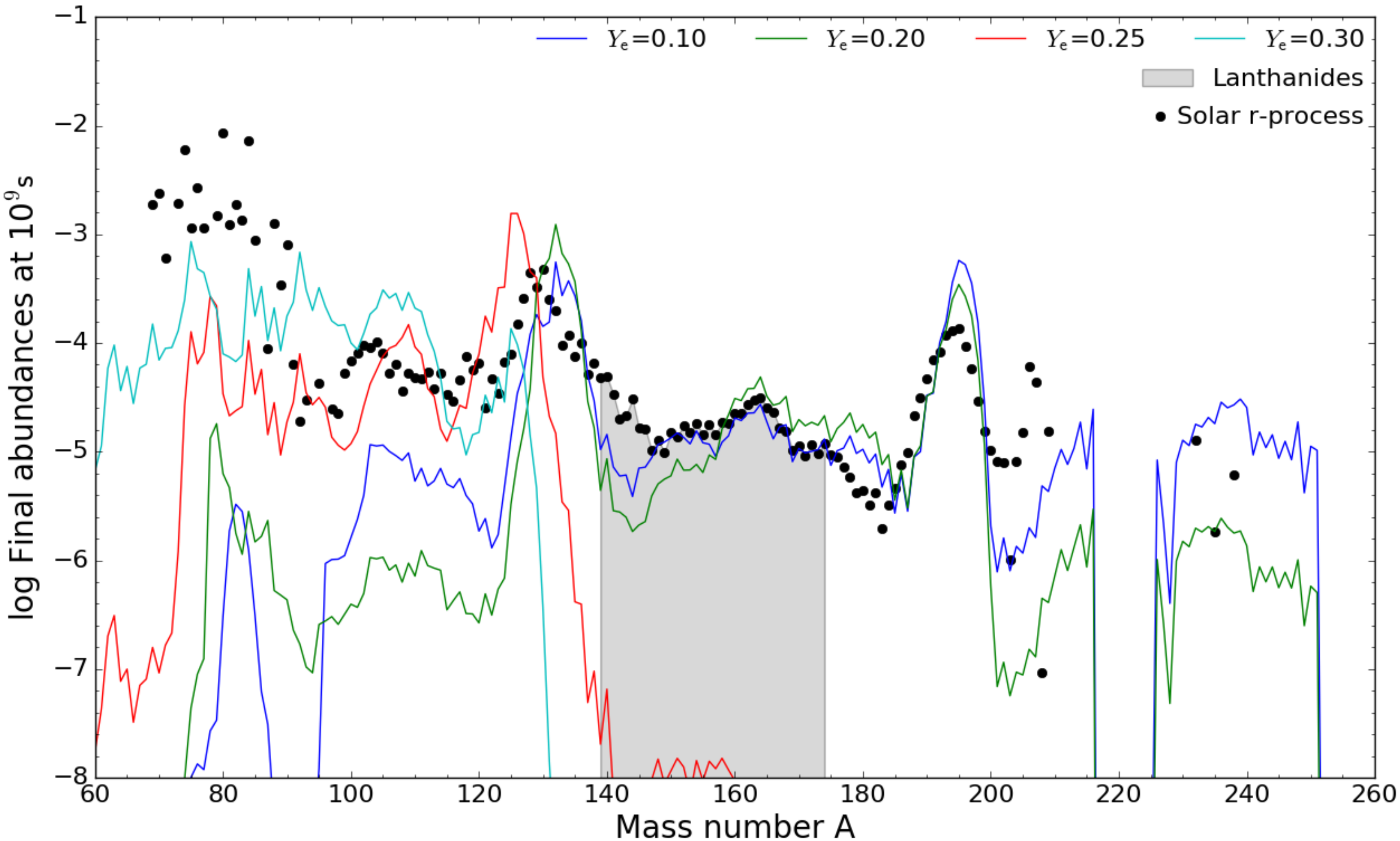

$Y_e < Y_{e,crit}$	$Y_e > Y_{e,cri}$
"robust" *r*-process A ≳ 130	"weak" *r*-process A ≲ 130
insensitive to details of trajectory	sensitive to details of trajectory

Nuclear heating rate

- Radioactive decays of *r*-process elements release nuclear energy

$$\dot{Q}_{r-process} = \sum_{i \in reactions} Q_i \lambda_i$$

$$with \quad Q = M_{initial} - M_{final}$$

$$\text{and} \quad \lambda = decay\, rate$$

$Y_e \gtrsim 0.25$	$Y_e \lesssim 0.25$
weak *r*-process (A<130)	robust *r*-process (A>130)
"blue transients" peaking after ~ 1 day	"red transients" peaking after ~ 1 week

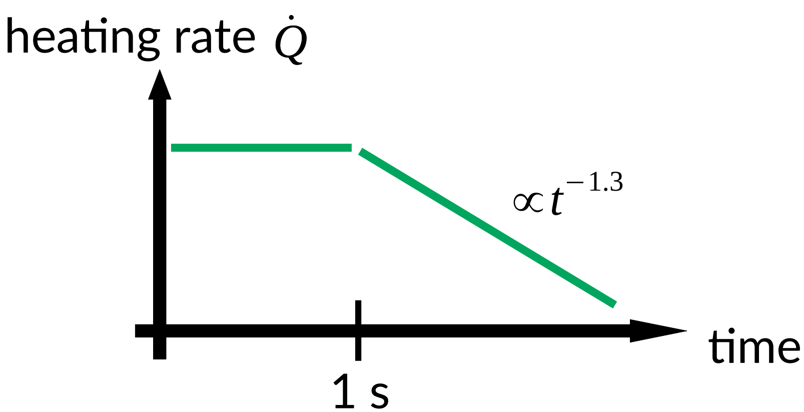

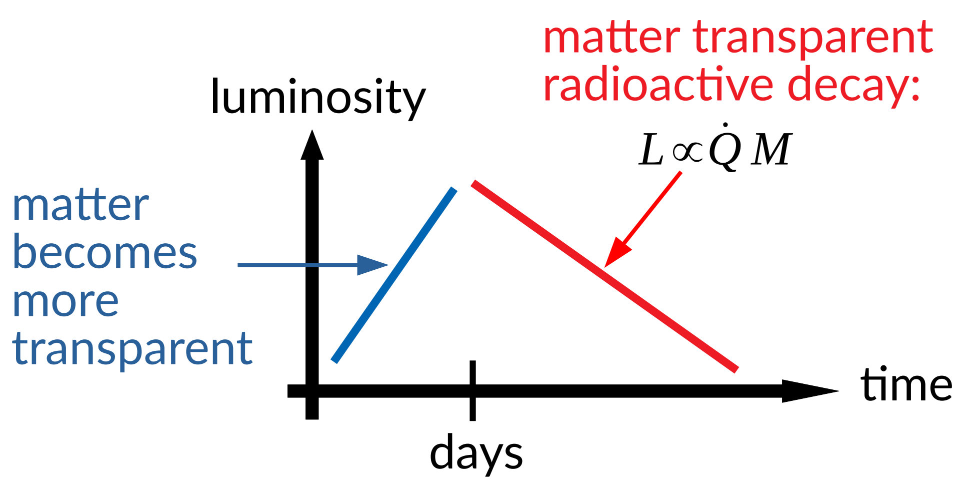

- key physics ingredients:
  1) ejecta mass, velocity, Y_e ➡ astrophysics
  2) opacity κ_γ ➡ atomic physics
  3) radioactive heating rate $\dot{Q}$ ➡ nuclear physics

Origin of He

- **Free neutrons** are abundant and provide an almost steady supply of free protons (through <u>*n*-decay</u>) and the efficient formation of deuterium (d) and tritium (t).
- Y_α <u>increases</u> through charge reactions such as t + t → 2n + ^{4}He and d + t → n + ^{4}He
- At later times (t >~ 2 s), α-<u>decay of translead nuclei</u> becomes significant and Y_α increases further

Perego, Vescovi+ 2020
arXiv:2009.08988

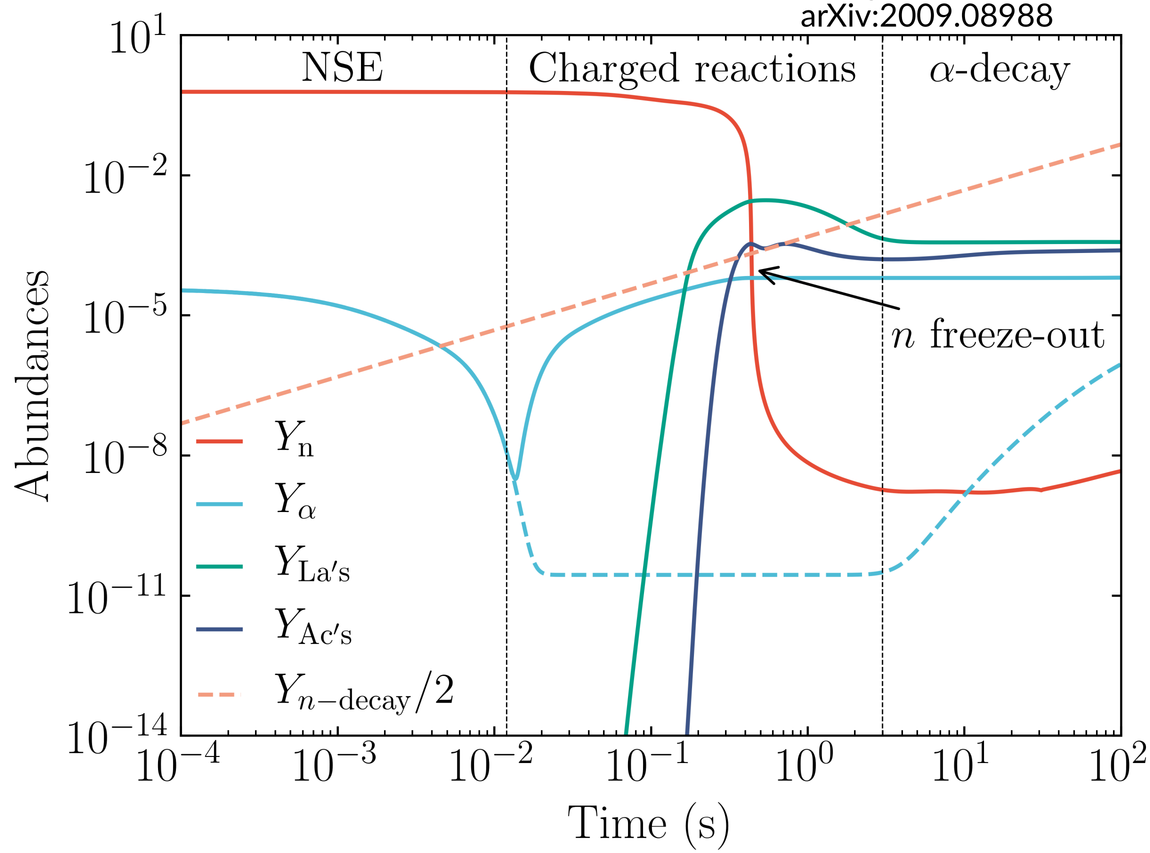

Trajectory with s = 10 k_B baryon^{-1}, τ = 10 ms and Y_e = 0.15